Accepted Manuscript

The S1P mimetic fingolimod phosphate regulates mitochondrial oxidative stress in neuronal cells

E. Martín-Montañez, J. Pavia, N. Valverde, F. Boraldi, E. Lara, B. Oliver, I. Hurtado-Guerrero, O. Fernandez, M. Garcia-Fernandez

PII: S0891-5849(19)30240-0

DOI: https://doi.org/10.1016/j.freeradbiomed.2019.04.022

Reference: FRB 14245

To appear in: *Free Radical Biology and Medicine*

Received Date: 12 February 2019

Revised Date: 3 April 2019

Accepted Date: 17 April 2019

Please cite this article as: E. Martín-Montañez, J. Pavia, N. Valverde, F. Boraldi, E. Lara, B. Oliver, I. Hurtado-Guerrero, O. Fernandez, M. Garcia-Fernandez, The S1P mimetic fingolimod phosphate regulates mitochondrial oxidative stress in neuronal cells, *Free Radical Biology and Medicine* (2019), doi: https://doi.org/10.1016/j.freeradbiomed.2019.04.022.

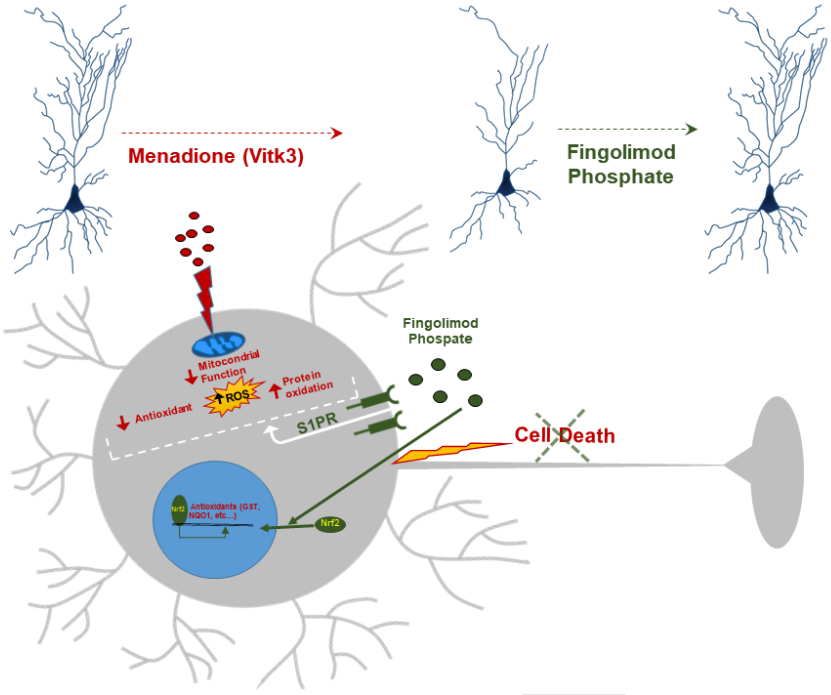

The S1P mimetic fingolimod phosphate regulates mitochondrial oxidative stress in neuronal cells.

E. Martín-Montañez[*#a], J. Pavia[*#a], N. Valverde[b], F. Boraldi[c], E. Lara[b], B. Oliver[d], I. Hurtado-Guerrero[d]. O. Fernandez[*#a], M. Garcia-Fernandez[*#b].

[a)] Department of Pharmacology and Paediatrics. Faculty of Medicine. Malaga University. Malaga. Spain.

[b)] Department of Human Physiology, Faculty of Medicine. Malaga University. Malaga. Spain.

[c)] Department of Life Sciences, University of Modena e Reggio Emilia, Modena, Italy.

[d)] Neuroscience Unit. Biomedical Research Institute of Malaga (IBIMA), Malaga University Hospital. Malaga Spain.

* These authors have equally contributed to this work

Authors for correspondence: emartinm@uma.es (E. Martín), pavia@uma.es (J. Pavia), oscar.fernandez.sspa@gmail.com (O. Fernandez), igf@uma.es (M. Garcia-Fernandez).

Abstract

Fingolimod is one of the few oral drugs available for the treatment of multiple sclerosis (MS), a chronic, inflammatory, demyelinating and neurodegenerative disease. The mechanism of action proposed for this drug is based in the phosphorylation of the molecule to produce its active metabolite fingolimod phosphate (FP) which, in turns, through its interaction with S1P receptors, triggers the functional sequestration of T lymphocytes in lymphoid nodes. On the other hand, part if not most of the damage produced in MS and other neurological disorders seem to be mediated by reactive oxygen species (ROS), and mitochondria is one of the main sources of ROS. In the present work, we have evaluated the anti-oxidant profile of FP in a model of mitochondrial oxidative damage induced by menadione (Vitk3) on neuronal cultures. We provide evidence that incubation of neuronal cells with FP alleviates the Vitk3-induced toxicity, due to a decrease in mitochondrial ROS production. It also decreases regulated cell death triggered by imbalance in oxidative stress (restore values of advanced oxidation protein products and total thiol levels). Also restores mitochondrial function (cytochrome c oxidase activity, mitochondrial membrane potential and oxygen consumption rate) and morphology. Furthermore, increases the expression and activity of protective factors (increases Nrf2, HO1 and Trx2 expression and GST and NQO1 activity), being some of these effects modulated by its interaction with the S1P receptor. FP seems to increase mitochondrial stability and restore mitochondrial dynamics under conditions of oxidative stress, making this drug a potential candidate for the treatment of neurodegenerative diseases other than MS.

Keywords

Fingolimod, Fingolimod Phosphate, Mitochondria, Oxidative stress, Neuroprotection, Antioxidant.

1. Introduction

Fingolimod is one of the few drugs available orally for treatment of Multiple sclerosis (MS), a chronic, inflammatory, demyelinating and neurodegenerative disease affecting the central nervous system [1–3]; showing a remarkable improvement in the clinical condition of the patients. Fingolimod produce its effects through the interaction of the drug with the sphingosine-1-phosphate (S1P) receptor [4–7], promoting a functional sequestration of T lymphocytes into lymphoid nodes. Studies on the effect of fingolimod have accumulated evidences, in addition to the well-documented regulation of the immune system, pointing to different mechanisms of action, other than the immunological, involved in the final effects of the drug; these include neuroprotective actions, mediated in part by their interaction with the neuronal S1P receptors [8]. In this sense there are works that indicate a neuroprotective effect of fingolimod [9,10] that could promote an improvement in cognitive function in ischemic processes [11] and neurodegenerative disorders like Huntington [12] or Alzheimer's disease [13,14].

In MS, inflammation, demyelination and neuronal and axonal damage are some of the pathophysiological mechanisms involved in the onset and progression of the disease [15] and in part, these injuries occur through mechanisms of oxidative stress [16]. Reactive oxygen species (ROS) play a crucial role in early and late stages of different neurological disorders [17–19]. The presence of inflammatory cells along with the production of inflammatory cytokines activate the generation of oxidative pathways. These species produced in inflammatory conditions, can cause important damage to macromolecules such as DNA, lipids and proteins.

Mitochondria is one of the main sources of ROS [20]; during the process of electron transport across the mitochondrial respiratory chain (MRC), a small percentage (less than 5%) of the electrons flowing through the chain, escapes and are attached directly to the O_2 forming anion superoxide ($O_2^{-\bullet}$) [21]. Given the high susceptibility of the central nervous system to ROS, it is worth thinking that oxidative stress, along with mitochondrial dysfunction, contribute significantly to the neurodegeneration in MS, as well as in other neurological disorders such as Parkinson's disease, Alzheimer's disease or Huntington [22,23]. To counteract an imbalance by high production of ROS, the cells use defence mechanisms, among others, antioxidant enzymes. This leads to think that maintaining or recovering REDOX homeostasis can be a therapeutic target in MS [24] and other neurological disorders that involve an increase in ROS [25].

In neurodegenerative diseases, including MS, ROS production depends mainly on high-producing enzymes expression in macrophages/microglia [26–28], which damages neuronal mitochondria [18,29,30] possibly by the production of oxidative damage in mitochondrial DNA [31]. In addition, the production of ROS

by mitochondria contributes to retrograde REDOX signalling from the organelle to the cytosol and nucleus [32,33].

In this paper, we will study the effect of fingolimod phosphate on the oxidative status, in a model of mitochondrial oxidative damage induced by menadione on neuronal cultures. In our opinion, fingolimod can exert its beneficial effect in MS and other neurodegenerative diseases not only through the modulation of the immune response, but also with the promotion of mechanisms for protection/repair of neuronal cell damage.

2. Material and Methods

2.1. Cell culture and treatments

Fingolimod phosphate is the active compound produced by phosphorylation of fingolimod in different tissues. In order to obtain a more tight control on the concentration of drug in the culture media, in this work we have used in all the incubations the active metabolite fingolimod phosphate (FP) kindly provided by Novartis, instead of the prodrug.

The SN4741 dopaminergic cell line derived from mouse substantia nigra [34] was cultured in D-MEM high glucose supplemented with 10% FCS penicillin-streptomycin, and L-glutamine (Gibco) to about 70-80% confluence. Cells were seeded in 100 mm^2 dish (5 millions) or glass botton 35 mm^2 dish and 6-well plates (200,000 each) and treated with different concentrations (5 and 15 µM) of menadione (vitamin K3, Sigma), a superoxide generating compound, in the absence or presence of 50 nM FP. The S1P receptor antagonists, W123 10 µM (Cayman Chemicals), was also co-incubated with menadione (Vitk3) and FP. The treatments were carried out in Locke's solution modified (137 mM NaCl, 5 mM $CaCl_2$, 10 mM KCl, 25 mM glucose, 10 mM Hepes, pH:7,4) supplemented with penicillin-streptomycin and L-glutamine during 2 to 6 hours. For confocal microscopy studies, immunocytochemistry, Giemsa and the measurement of mitochondrial oxygen consumption, dishes, plates and coverslips were pre-coated with 100 µg/mL of poly-D-lysine.

Additional experiments were performed to assess the effect of FP in the recovery of the oxidative damage produced. In these experiments, after incubation of two hour with Vitk3, the buffer was changed by, only buffer (in control cells) or buffer whit 50 nM FP (treated cells) and the same but in presence of 10 µM W123 to clarify the contribution of the S1P receptor on this recovery.

2.2. Cell viability

Viability was determined by quantifying the release of the intracellular enzyme lactate dehydrogenase (LDH, EC 1.1.1.27) [35]. The LDH levels were measured

in cell-free culture supernatants using a commercial spectrophotometric assay kit (Randox Laboratories Ltd., UK) adapted to a Cobas Mira Autoanalyser (ABX Diagnostics, France). The results are expressed as the percentage of LDH released into the medium relative to total LDH (medium and cells lysed using Triton X™-100). For morphology studies, cells were fixed in 100% methanol and stained with Giemsa (Merck). Cells were examined for nuclear, cytoplasmic and cell membrane changes.

2.3. Caspase activation assay

Caspase-3 cleavage was used to study apoptosis. Compounds (Vitk3, FP, and W123) were mixed in Locke's solution modified and pipetted into wells together with 5 µM NucView® 488 caspase-3 substrate (Biotium) and incubated at 37 ºC. Staurosporine was used as a positive control (data not shown). Images were acquired using a fluorescence Nikon Eclipse Ti inverted microscope. Fluorescence analysis was performed by using FIJI program (ImageJ software US National Institute of Health; http://imagej.nih.gov/ij/)

2.4. Determination of mitochondrial levels of ROS

Mitochondrial ROS production was estimated by measuring $O_2^{-\bullet}$ production via flow cytometry using MitoSOX™ Red (Molecular Probes), according to previously published procedures [36,37]. Prior to the end of the incubation period, the cells were labelled with 2.5 µM MitoSox for 30 min at 37 °C. The cells were then washed and immediately analysed via flow cytometry using the 585/40 nm (FL2) filter in an Accuri™ C6 flow cytometer (BD biosciences). Ten thousand events (cells) were recorded and evaluated using FCS Express 5 software (De Novo Software).

2.5. Preparation of homogenised cells

The cells were suspended in buffer containing 10 mM HEPES, 10 mM KCl, pH 7.4, a protease inhibitor cocktail and phosphatase inhibitors (Sigma), incubated at 0 °C for 20 min and homogenised in the presence of 0.01% digitonin. The Bradford protein assay was used to measure the concentration of total protein in the samples [38].

2.6. Antioxidant enzyme activity

NQO1 activity (EC 1.6.99.2) was measured as described elsewhere [39] by following the decrease in NADH absorbance at 340 nm adapted to a Cobas Mira Autoanalyzer. The reaction mixture at a final volume of 200 µL contained 25 mM Tris·HCl (pH 7.5), 0.01% Tween 20, 0.7 mg/mL BSA (pH 7.4), 40 µM menadione, 5 µM FAD, 200 µM NADH, and cell extract. Measurements were made at 25 seconds intervals over a time period of 10 min. One activity unit was defined as the oxidation of 1 µmol NADH to NAD/min at 37 ºC.

GST activity (E.C.2.5.1.18) was determined spectrophotometrically at 340nm by measuring the formation of the conjugated of glutathione and 1-chloro-2,4-dinitrobenzene (CDNB). One unit is the amount of enzyme that catalyses the formation of 1 µmole of S-2-2,4-dinitrophenylglutatione per minute at 37ºC using 1mM concentration of GSH and CDNB.

2.7. Markers of oxidative stress

2.7.1. Determination of homogenates sulfhydryl groups (total thiol).

Cell homogenate sulfhydryl (-SH) groups were determined by using Ellman's reagent 5,5′-dithiobis(2-nitrobenzoate)-DTNB adapted to Cobas Mira [36]. Sample (10 µL) was mixed with 200 µL of 0.1 M Tris buffer, containing 10 mM EDTA, pH 8.2. The absorbance at 405 nm, given by the sample alone, was subtracted from that obtained from the same sample 10 min after addition of 8 µL of 10 mM DTNB. A blank containing only DTNB was also included, and -SH concentration was calculated by using a standard curve of glutathione. Intra- and inter-assay variation coefficients were 1.2% and 6%, respectively.

2.7.2. Determination of advanced oxidation protein products (AOPP).

AOPPs were evaluated using a microassay adapted to Cobas Mira [40]. Briefly, 18 µL of sample or chloramine-T (ch-T) standard solutions (400–6.25 µmol/L) were placed in each well of the Cobas Mira autoanalyser followed by addition of 200 µL of reaction mixture, consisting of 81% phosphate buffer solution (PBS), 15% acetic acid, and 4% 1.16 mM potassium iodide. Absorbance was read at 340 nm (the blank contained PBS instead of sample). AOPP concentration was obtained based on measured ch-T equivalents.

2.8. Electrophoresis and Western blot

The samples were resuspended in (5X) polyacrylamide gel electrophoresis (SDS-PAGE) loading buffer and boiled at 100 °C for 3 min using a thermo-block. The samples were then loaded (15 µg of protein/well) on a 12% polyacrylamide gel and subjected to a constant current of 130 V for one hour. The transfer was performed using a semi-dry transfer device (Trans-Bolt Turbo™, Bio-Rad) to a nitrocellulose membrane with a pore size of 0.45 µm (current intensity: 0.8 mA/cm^2 for 7 min). After blocking (TBS/twin/0.5% fat free milk), the membranes were incubated in various primary antibodies (produced in rabbit) at different dilutions (Trx2 (1:500 v/v) from Santa Cruz Biotechnology, anti-β-actin (1:1000 v/v) and Nrf2 (1:500 v/v) from Cell signalling technology and anti-Heme-oxygenase-1 (1:1000 v/v) Calbiochem) for 12 h at 4 °C, followed by incubation for 1 h with anti-rabbit IgG alkaline phosphatase conjugated secondary antibody (Sigma) at a 1:10000 v/v dilution. The final colour reaction was developed using nitro blue tetrazolium/5-bromo-4-chloro-3-indolyl phosphate (NBT/BCIP). The Western blots were digitised using a flatbed

scanner (HP Scanjet 5500c, Hewlett-Packard) and analysed using ImageJ software (US National Institute of Health; http://imagej.nih.gov/ij/).

2.9. Measurement of mitochondrial markers

2.9.1. Mitochondrial membrane potential

Mitochondrial membrane potential (MMP) was evaluated using the lipophilic cationic probe 5,5,6′,6′-tetrachloro-1,1′,3,3′-tetraethylbenzimidazolcarbo-cyanine iodide (JC-1) according to a previously described procedure [41]. JC-1 is a lipophilic carbocyanine that exists in a monomeric form and accumulates in mitochondria. In the presence of a high MMP, JC-1 reversibly forms aggregates that, after excitation at 488 nm, fluoresce in the orange/red channel (FL2-590 nm). Collapse of the MMP provokes a decrease in the number of JC-1 aggregates and a subsequent increase in monomers that fluoresce in the green channel (FL1-525 nm). This phenomenon is detected as a decrease in orange/red fluorescence and/or an increase in green fluorescence. The MMP was estimated from the red/green ratios as the FL2/FL1 ratio of JC1 staining by flow cytometry. Thus, cells were incubated in 1 µg/mL JC-1 for 20 min at 37 °C, rinsed twice, detached and immediately analysed using FL1 and FL2 filters in an Accuri^{TM} C6 flow cytometer (BD biosciences). Ten thousand events (cells) were recorded and evaluated using FCS Express 5 software (De Novo Software). To completely deplete the MMP, the potassium ionophore valinomycin (1 µM) was used as control.

2.9.2. Determination of cytochrome c oxidase (COX) activity

COX activity (EC 1.9.3.1) in cell homogenates was assessed using a COX assay kit adapted to a Cobas Mira Autoanalyzer [42]. This assay is based on observation of the decrease in absorbance at 550 nm of ferrocytochrome c caused by its oxidation to ferricytochrome c by cytochrome c oxidase. One unit was defined as the oxidation of 1.0 µmol of ferrocytochrome c per minute at pH 7.0 and 37 °C.

2.9.3. Mitochondrial oxygen consumption rate

Mitochondrial oxygen consumption rate (OCR) was measured using a Seahorse Bioscience XF24 analyzer (Agilent) in the specific 24-well plates at 37°C, with correction for positional temperature variations adjusted from 4 empty wells evenly distributed within the plate [43]. Cells were seeded at 20,000 cells per well during 18 h prior to the analysis and each experimental condition was performed on 8 replicates. Before each measurement, the cells were washed and 590 µL of Agilent Seahorse XF Base Medium without phenol red was added to each well. After a 15 min equilibration period, 3 successive 2 min measurements were performed at 3 min intervals with inter-measurement mixing to homogenize the oxygen concentration in the medium, and each condition was measured in independent wells. Concentrated compounds (10X)

were injected into each well by using the internal injectors of the cartridge and 3 successive 2 min measurements were performed at 3 min intervals with inter-measurement mixing. Measurements were normalized according to protein concentration in each well.

2.10. Measurement of mitochondrial distribution

The green-fluorescent mitochondrial stain MitoTracker™ Green FM (MTG) (Molecular Probes) was used to localize the mitochondria after treatments [44]. Cells were incubated in 75 nM MTG for 30 min at 37 °C, rinsed and observed under a confocal microscope LEICA SP5 II (Wetzlar) with excitation at 488 nm and emission at ~530 nm.

2.11. Electron microscopy

Two independent sets of experiments were performed for morphological analyses. Cell pellets were processed as described previously with some modifications [45]. Briefly, samples were fixed in 2.5% glutaraldehyde (Electron Microscopy Sciences) in 0.1 M cacodylate buffer and postfixed with 1% osmium tetroxide. Cell pellets were gradually dehydrated in ethanol series (30%, 50%, 70%, 95% and 100%) and then embedded in Araldite (Serva Electrophoresis). Ultra-thin sections (70 nm) were cut and collected on 150 mesh copper grids and stained with UranyLess (Electron Microscopy Sciences) followed by Reynolds lead citrate staining. Sections were examined with a FEI NOVA NanoSEM 450 and images were obtained using the STEM mode using Solid State Detector with voltage at 30 kV.

2.12. Immunocytochemical Staining

Cells were fixed by adding methanol previously chilled at -20 °C and incubating the plate at -20 °C for 20 min. The wells were washed with PBS and coverslips were removed and incubated with Nrf2 primary antibody (1:50 v/v) Santa Cruz Biotechnology in PBS/3% BSA/0.02% sodium azide at 4°C over-night and thereafter incubated with a fluorescent secondary antibody Alexafluor™ 488 (2 drops/mL) (Life technologies), in PBS/BSA for 30 min at room temperature in the dark. Coverslips were mounted with Fluoromount™ (Sigma) and images were acquired using a confocal microscope LEICA SP5 II (Wetzlar) with excitation at 488 nm and emission at ~530 nm and processed using the software LAS AF Lite (Leica).

2.13. Statistical analysis

Statistical differences were determined using one-way ANOVA. Pairwise comparisons were performed using a post hoc Newman-Keuls multiple comparison test. Statistical significance was considered to be $p<0.05$. For data in which the measured units were arbitrary, the respective values represent the percentage relative to the control value unless specified.

3. Results and Discussion

In the last years, evidence has accumulated suggesting a major role of oxidative stress in the pathogenesis of neurodegenerative diseases, including MS [46,47], being implicated as mediators in demyelination and axonal damage. Antioxidants could be thus considered as therapeutic tools in these diseases in which could prevent the propagation of tissue damage, improving survival and neurological outcomes [48,49]. In this context, we have studied the antioxidant profile of fingolimod in a model of mitochondrial oxidative damage induced by menadione (Vitk3), a ROS generator in mitochondrial compartment [50], on neuronal cultures.

The FP concentration chosen has been based in experiments on the toxicity of the drug in a range from 0.1 to 100 nM on control cultures where no damage was seen (data not shown). In other set of experiments, different concentrations of FP were tested for the ability to protect neuronal cultures against the damage produced by 15 µM Vitk3, assessed by cell viability (Fig. 1a). The dose chosen in this study (50 nM FP) was the most effective preventing cell death. In the analysis of the Giemsa stained images of Vitk3 treated cells compared to control (Fig. 1 c2 and c1), we found a great heterogeneity in cell size and shape, with shrunken condensed pyknotic nuclei. Some cells show a loss of plasma membrane integrity with poor interconnections and loss of neuronal processes as well as different degrees of swelling (Fig. 1 c2). When 50 nM FP is present in the treatment media, cells recover a morphology similar to control cells. Although a few of them still show nuclear condensations, they tend to stablish interconnections and shape and size become similar to control cells (Fig. 1 c3). The effect of FP on cell morphology is reverted when the S1P antagonist W123 (10 µM) was included in the incubation media (Fig. 1 c4).

We have investigated the mitochondrial production of ROS in neuronal cultures after treatment with Vitk3 in presence or absence of 50 nM FP to evaluate its antioxidant effect. In these experiments, we have found an increase in mitochondrial ROS production after treatment whit Vitk3 compared to control which returns to near control levels in presence of FP (Fig. 1b)

This dose was also evaluated at the electron microscopy (EM) level (Fig. 2); in these experiments, we have analysed the ultrastructural morphology of neurons after various treatments. Untreated cells (CO) showed an ovoid or round shape. In general, nuclei possess indented zone and contain at least one large nucleolus. The cytoplasm displayed free ribosomes, elongated/sinuous cisterns of endoplasmic reticulum. The cisternae of Golgi stacks were well organized. The deleterious effect of Vitk3, leading to cell damage an death can also be observed at the electron microscopy level, where Vitk3 (4h of incubation) induce ultrastructural alterations in the cells. These are extremely heterogeneous with respect to both shape and size, indicating alterations of the cellular cytoskeleton and in some peripheral cytoplasmic area dilated cisterns of endoplasmic reticulum (ER) can be observed. Nuclei rarely display a nucleolus and large

area of the cytoplasm are poor in organelles with a significant reduction of ER and mitochondria number, as will be commented later. The Golgi apparatus is rarely observed and the cisternae are fragmented. Moreover, a few cells showed a loss of plasma membrane integrity. In these experiments, we do not see a typical morphology of apoptosis; as seen in caspase-3 activation experiments (Fig. 4), probably because instead of a clear apoptotic process, we are facing a mixture of different processes recently denominated regulated cell death (RCD) [51,52], including apoptosis, ferroptosis and necrosis among others, as described recently in pathologies characterized by cell death and inflammation, such as some neurodegenerative diseases including MS [53,54]. When Vitk3 and FP are combined, the cells showed an improvement in its morphology. The cells show electron-dense chromatin balls and in the cytoplasm, some normal mitochondria can be found. Small Golgi apparatus and ER tubules shorter than the previous condition are observed.

The morphological damage found at EM, is probably induced by the increase in ROS production promoted by Vitk3, which involves an imbalance in oxidative stress, and is prevented by FP (Fig 1b). When we studied the advanced oxidation protein products (AOPP), a marker of oxidative damage (Fig 3a), Vitk3 increases by 35.2% the levels of AOPP compared to control. This increase returns to near control levels after co-incubation with FP. Furthermore, we have also found a beneficial effect of FP in the cellular antioxidant pool of total thiols (Fig 3b), where incubation with Vitk3 produces a decrease of 46.7% compared to control; reduced to only 21.1% after co-incubation in presence of FP. The decrease in total thiols could promote a malfunctioning of GST, GPX4 and/or other key enzymes involved in the detoxification of products induced by ROS that in turn, could cause neuronal damage contributing to RCD processes as seen in some neurodegenerative diseases including MS [54,55]. Although our approach is based in a model of mitochondrial damage and not in a MS model, this effect is similar to that found in animal models of MS [54] and in relapsing remitting multiple sclerosis (RRMS) patients taking fingolimod, where a decrease in oxidative markers compared to newly diagnosed patients without immunomodulatory therapy was found [56].

The increase in mitochondrial ROS production also induces the activation of caspase-3. In our experiments, FP reduces the caspase-3 activation induced by Vitk3 (Fig 4), although we have been unable to demonstrate clear differences in caspase-3 western blot experiments, agreeing with the Giemsa staining experiments, where not all cells showed a classic apoptotic morphology. The decrease in caspase-3 activation promoted by FP could be attributed to the improvement in mitochondrial dynamics as seen by EM, mitochondrial ROS production and caspase activation experiments. The same applies to PAPR1 western blot experiments, where we were unable to see clear differences (data not shown).

Mitochondrial damage has been proposed as one of the mechanisms involved in the pathogenesis of neurodegenerative diseases including MS, mainly focused on the production of oxidative molecules [18,22,33] and then, the

mitochondrial targeted antioxidants could be considered as a good strategy for the treatment of MS damage [57]. In order to evaluate the mitochondrial targeted antioxidant effect of FP we have studied the mitochondrial morphology, distribution and function, after treatment with Vitk3 in presence or absence of 50 nM FP in neuronal cells cultures.

Morphologically in EM experiments, CO cells showed mitochondria not dispersed into cytoplasm but localized in discrete area of the cells with orthodox configuration. After treatment with Vitk3 (4h), almost all the mitochondria show ultrastructural alterations at the electron microscopy level, such as thin cristae and distorted/disrupted cristae in rarefied matrix. A subset of mitochondria also exhibit cristae stacks indicating a loss of connectivity to the inner membrane. In some cases mitochondria exhibit swelling with or without highly electron contrasted membranous whorls. Whorls formations can be the results of repetitive autophagy events linked to lipid peroxidation. When Vitk3 and FP are combined, normal mitochondria can be found in the cytoplasm, although we still can find mitochondria with variable size due to swelling with reduction or disrupted cristae (Fig 2 insert).

Mitochondrial cellular distribution changes under stress conditions and when its integrity are damaged (ie. oxidative stress unbalance). Healthy mitochondria are evenly distributed in soma and axons, with certain predominance in areas where energy is required (pre and postsynaptic), and are also important along the axon, where they serve to maintain the degree of polarisation needed to transmit the action potential and as calcium regulator [58]. Unhealthy mitochondria remain closer to the nucleus without reaching more peripheral areas of the cells; furthermore, damaged mitochondria are transported back, close to the cell body, where lysosomes and other organelles, needed to degrade mitochondria, are more abundant [59]. Our experiments with MTG to study distribution (Fig 5), showed a change in the network pattern, going from normal fusiform structures evenly distributed and found as a filament shape in neuronal body and axons of control cells, to a more disorganized structure of swelled and sphere shaped mitochondria in Vitk3 treated cells. Co-incubation with FP partially recovers the localization of mitochondria within axoplasm, which is necessary to axonal function.

Functionally, as can be seen in figure 6a, incubation of cells with Vitk3 produces a dramatical decrease (43.7 %) in MMP compared to control; this can be almost totally reverted by the co-incubation of Vitk3 in presence of FP. One explanation for the decline in MMP can be the formation, induced by Vitk3/ROS, of mitochondrial transition pores (mPTP) [50] which impairs morphology, function and distribution in axons and body cells [60]. The recovery in the MMP promoted by FP acting as a S1P mimetic, could be related with the interference in the formation/maintenance/opening of mPTP. Interestingly mPTP has been involved in the axonal damage found in MS and other neurodegenerative diseases [60].

MMP and COX, the main regulator enzyme complex of the mitochondrial respiratory chain, are linked in healthy and pathological situations. In healthy situations, COX activity maintain the MMP at normal levels (~120 mV) sufficient for efficient energy generation. In pathological situations, a decrease in COX activity (such as in acute inflammation) leads to a decrease in MMP and energy depletion; and the increase in COX activity (such as in ischemia/reperfusion), increases MMP and triggers ROS production, damaging the cell and leading to cell death [61].

In our work, we have found a 20.7 % decrease in COX activity after incubation with Vitk3, again this effect was counteracted with the co-incubation of cultures in presence of FP, restoring COX activity to control levels (Fig 6b). The decrease in COX activity could be due to an increase in ROS production triggered by Vitk3, as seen by others [62]. Also, a decrease in COX activity produced by the increase in ROS generated in inflammatory processes, has been reported in MS and other neurodegenerative diseases [63,64]. In this sense, FP contributes to a decrease in ROS production, as commented above, that could be related with the restoring in COX activity. We could speculate that the restoring in COX activity would be produced by an increase in intracellular S1P induced by the inhibition of S1P lyase by FP [65]; which in turns would bind to prohibitin 2 which regulates complex IV assembly and respiration [66]. We have also found an involvement of the S1P receptor, at least in part, in the normalizing of COX activity and mitochondrial function (see later and Fig 15) agreeing with other authors [67]. Although we cannot exclude an effect of FP through its receptor modulating the phosphorylation of kinases (pAkt/Akt) that would phosphorylate pro-apoptotic factors such as Bad, which would ultimately decrease mitochondrial stress, as has been seen in other models of mitochondrial toxic damage (MPTP/MPP+) [68].

COX is the enzyme at the final respiratory chain complex where over 90% of oxygen is consumed [69]. The oxygen consumption is the major marker of mitochondrial function and cell survival; in this work we have performed experiments to assess the effect of FP on oxygen consumption during the incubation with Vitk3 (Fig 7). Incubation of cultures with Vitk3 triggers initially an increase in oxygen consumption, but at longer periods this consumption decreases dramatically (61% after 4 hours). This, along with the decrease found in MPP could indicate that cells are in RCD processes as mentioned before. When the experiments were performed co-incubating Vitk3 in presence of FP, the decrease found in OCR was reduced to only 17%, indicating that at long co-incubation periods, FP promotes a functional mitochondrial recovery, according to the morphological changes seen in EM. The oxidative damage induced by Vitk3, can be counteracted by FP as seen by the recovery in the MMP and COX activity mentioned above, pointing to a mitochondrial protective effect promoted by FP found in this work and in others [70,71].

The RCD mechanism activated in the early phase after incubation with Vitk3 (1 to 2 hours) could be based in a mitochondrial stimulation, traduced in an increase in mitochondrial respiration (Fig 7), COX activity and MMP (Fig 8a and b), which leads to an increase in mitochondrial ROS production. This process could be similar to that found in initial stages of some neurodegenerative diseases such as MS [72]. We could postulate that the RCD modulation produced by FP would focus on the decrease in this mitochondrial stimulation, which in turns would decrease mitochondrial ROS production and diminish RCD processes, probably by interfering in the mPTP formation as commented before. At the confocal microscopy level, in this early phase, the mitochondrial distribution studies with MTG (Fig 9) showed an initial change in the network pattern. In control cells, we found normal fusiform structures evenly distributed and found as a filament shape in neuronal body and axons. Cells treated with Vitk3 showed a more disorganized structure of swelled and sphere shaped mitochondria, more evident in the neuronal body than in axons. Co-incubation with FP partially recovers shape and localization of mitochondria within axoplasm giving a pattern more similar to that found in control cells.

To counteract the excess in ROS production, the cells have many transcription factors involved in the maintenance of mitochondrial homeostasis and structural integrity, being Nrf2 particularly important under conditions of oxidative, electrophilic/inflammatory stress and neurodegeneration [73]; among other actions, promoting the maintenance of glutathione in its reduced state [74]. Nrf2 regulates the expression of more than 250 genes involved in antioxidant actions [75]. The importance of this factor is based in its effect counterbalancing mitochondrial ROS by regulating antioxidant enzymes, such as GST, NQO1, HO1 and Trx2 and maintaining thiol groups in its reduced state.

In our western blot experiments, incubation of cells with Vitk3 produces a decrease in Nrf2 of 23% compared to control (Fig 10a). When co-incubated in presence of FP, the effect of Vitk3 was reverted, generating an increase in Nrf2 of 11% compared to control. Interestingly, cells incubated with FP in absence of Vitk3 showed an increment in Nrf2 of 38% compared to control. The effect of FP on Nrf2 seems not to be mediated by the S1P receptor; as it is not modified by the co-incubation with the S1P antagonist W123.

One tentative explanation to these findings would be that Vitk3 induce a decrease in Nrf2 levels either by decreasing its synthesis or by increasing its degradation [76,77] (Fig 10 b2). When FP is present in the incubation media, the levels of Nrf2 are maintained with a notable nuclear translocation (Fig 10 b3), in an attempt to protect against the oxidative damage by triggering the synthesis of protective enzymes. When the cells were incubated with FP in absence of Vitk3, Nrf2 levels are increased, and this would favour the nuclear translocation that we see when Vitk3 is present in the media [78] (Fig 10 b4).

The Nrf2 recovery could be related with an improvement in bioenergetics on the neurones mediated by an increase in COX activity regulating MMP and oxygen consumption, agreeing with the results shown in figure 6 and 7 respectively [73]. This effect could be of great importance in neurodegenerative pathologies including MS, where a decrease in Nrf2 levels has been found in grey matter, correlated with an increase in oxidative damage and mitochondrial respiratory enzymes [58,79]. Nrf2 also regulates several phase II enzymes, among them GST and NQO1, working as detoxifiers of several toxic substrates produced by ROS and involved in the pathogenesis of different neurodegenerative diseases [80–82]. In our experiments, we have found that the incubation of cells with Vitk3 produce a decrease in both, GST and NQO1 activity compared to control. Co-incubation with FP restore the activity to values close to those found in control cells, in the case of NQO1, this recovery goes to values even higher than control (Table 1), agreeing with the Nrf2 western blot experiments, where FP is able to increase the levels in absence of Vitk3 to values higher to those found in control cells. Both enzymes are also related with the protective effect of other drugs used in the treatment of MS and other neurodegenerative diseases [48,80,83].

Enzyme assayed	Control	Vitk3	Vitk3+FP	FP
GST (mU/mg protein)	29.4±3.5	20.8±3.3*	25±3$^{\&}$	30±3.6
NQO1 (U/mg protein)	0.4±0.05	0.15±0.02*	0.6±0.07$^{\&}$	0.6±0.06*

Table 1: Activities of enzymes involved in detoxifying toxic substrates produced by ROS. Data were combined from 3 to 4 independent experiments and presented as mean ± SEM. (*$p<0.05$ versus control; & $p<0.05$ versus Vitk3).

Nrf2 is also involved in the up regulation of other antioxidant factors, such as HO1 and Trx2. HO1 is a protective molecule generated by neuronal tissue as response to a variety of toxic and traumatic stimuli, such as brain damage and spinal cord injury [84]. In our western blot experiments, we have found a decrease of 27% in HO1 levels compared to control after incubation of the cells with Vitk3, again, co-incubation with FP restores the HO1 values to those found in control cells (Fig 11a). Trx2 is related with neurodegenerative processes [85]; it is a small mitochondrial redox protein that is essential for the control of mitochondrial ROS homeostasis, RCD and cell viability. It is expressed in regions whit high energy demand and high rate of production of oxidized metabolites, such as substantia nigra and subthalamic nucleus [86]. In our western blot experiments, incubation of cells with Vitk3 produces a decrease of 44% compared to control and again the co-incubation with FP restores Trx2

levels close to control (7% less than control) (Fig 11b). The last action mentioned for Nrf2 is related with the maintenance of thiol in its reduced state; in this sense, we have found a decrease in the total thiol groups after incubation with Vitk3, as mentioned above (Fig 3b), that can be partially reverted by co-incubation with FP. These effects would be related with the ability of FP to inhibit sphingosine kinase 1 which in turns would increase Nrf2 and phase II related enzymes [87].

Once the mitochondria has been converted in a source of ROS after incubation with Vitk3, we have performed a couple of pilot experiments to see the recovery in function/morphology. In these experiments, cells were incubated during two hours with Vitk3 in presence or absence of FP. After that time, Vitk3 was removed from the media and cells were incubated four additional hours in the following conditions: two groups were incubated with media (Vitk3 and control), and one with FP 50 nM and then, the bioenergetics (OCR) and morphology (MTG and electron microscopy) experiments repeated. Although we are aware that we are far from an MS model, we decided to maintain FP in the media of one group because it has been reported that withdrawal of fingolimod triggers the damage again in RRMS patients [88,89].

In the OCR experiments, cells treated with Vitk3 and incubated four additional hours in media, maintain the increment in levels of oxygen consumption, about 20% compared to control; whereas in cells co-incubated with FP, the oxygen consumption values returns to levels similar to control cells (Fig 12). Interestingly, in these experiments FP was able to restore the values to control levels, whereas in the previous OCR experiments (Fig 7) the recovery was less evident (20% less than control).

Regarding morphology, at the electron microscopy level, ultrastructural alterations become less pronounced than those seen in 4 hours of incubation. When VitK3 and FP are combined, the cells show intermediate characteristic, the majority of nuclei shows at least one nucleolus. Cells displayed a shortened of the Golgi stacks and tubulo-vesiculated clusters. The number and morphology of mitochondria/cell is similar to control, however some mitochondria demonstrate a variable morphology appearing with both intact and disrupted cristae and some swelling (Fig 13).

In MTG experiments, cells incubated with Vitk3 produce swollen mitochondria, as they keep being a source of ROS inducing self-damage, whereas co-incubation with FP reverts partially the changes promoted by Vitk3; mitochondria are less swollen and closer to the axons in these cells (Fig 14); furthermore, they recover almost totally their function as seen in the OCR experiments. Although our model is based in a mitochondrial oxidative damage, the effect of FP on mitochondria found in this work, could be related with the clinical findings on relapse after withdrawal of fingolimod in MS patients [88,89]. Mitochondrial mobility can be regarded as an index of health, as malfunction can affect it. As mentioned above, healthy mitochondria are evenly distributed in

soma and axons, especially in areas where energy is required (pre and postsynaptic), and along the axon, where they serve to transmit the action potential and as calcium regulator [58]. Unhealthy mitochondria, as a result of residual damage induced by Vitk3, remain closer to the nucleus; furthermore, damaged mitochondria are transported back, close to the cell body. The changes in mitochondrial pattern distribution in neuronal compartments could be regarded as a target for treatment and improvement of neuronal function in patients with neurodegenerative diseases such as MS [90].

In order to see the involvement of the S1P receptors in the FP effects shown above, we have performed the same experiments in presence of the S1P antagonist W123.

We have found that S1P receptors are involved in the majority of the mitochondrial protective effects of FP. It reverts at least partially the RCD (Fig 1c and 15b) processes triggered by the increase of ROS induced by Vitk3 (Fig 15a) and consume of antioxidant reserve (TTL) (Fig 15c). The FP effects on MMP and COX activity and OCR (Fig 15 d, e and f respectively) seems to be mediated also by S1P receptors, as can be totally abolished by co-incubation in presence of the S1P antagonist W123; also found by others in neuronal and non-neuronal cells [67,91]. FP would also interact as S1P mimetic with mitochondria prohibitin 2 which regulates complex IV assembly and respiration [66]; this effect is also mediated by S1P receptors as can be abolished by co-incubation with W123 [91]. Regarding neuronal mitochondrial distribution, we have found similar results; FP treatment restores the anomalous distribution of mitochondria promoted by Vitk3 to a more normalized pattern with mitochondria more evenly distributed in axons and body. All the above mentioned, points to an essential role played by the S1P receptor in the maintenance of mitochondrial homeostasis.

Conclusions

From our work, we can conclude that FP has a protective effect on the oxidative imbalance produced by mitochondrial ROS toxicity. According to this mechanism, FP would exert its actions not only in the early phase of the damage but also in more advanced stages, where mitochondria are damaged and dysfunctional, and this action would be added to the effect as an immunomodulator demonstrated by other authors. FP seems to increase mitochondrial stability and restore mitochondrial dynamics under conditions of oxidative stress, making this drug, apart from the therapeutic efficacy already demonstrated in MS, a potential candidate for the treatment of other neurodegenerative diseases.

Acknowledgements

We wish to thanks Dr. Ernest Arenas for providing SN4741 cells, Francisco David Navas-Fernández and Manuela Vega-Sánchez for the assistance in the microscopy and imaging analysis and Vanessa de Luque for technical assistance.

This research was supported by the following projects: PS13/14: Study of the non-immunological mechanisms of action of Gilenya (Fingolimod) as therapeutic tool in Multiple Sclerosis and/or other neurodegenerative diseases. Novartis Farmacéutica S.A.; CTS507 and CTS156 from Consejería de Economía Innovación Ciencia y Empresa, Junta de Andalucía and Plan Propio de la Universidad de Málaga 2016. N.Valverde was supported by the Programa operativo de empleo juvenil; Junta de Andalucía and Fondo Social Europeo (EU).

Author contributions

J. Pavía, O. Fernández, M. García-Fernandez and E. Martín-Montañez designed and supervised the study. M. García-Fernandez and E. Martín-Montañez optimized the oxygen consumption experiments. J. Pavía and E-Martín-Montañez performed the western blot experiments. F. Boraldi performed the electron microcopy experiments. N. Valverde, E. Lara, B. Oliver, and I. Hurtado-Gerrero performed experiments. M. García-Fernandez, J. Pavía, O. Fernandez and E. Martín-Montañez wrote the paper with contribution from all authors.

Competing interest

Oscar Fernandez received honoraria as consultant in advisory boards, and as chairmen or lecturer in meetings, and has also participated in clinical trials and other research projects promoted by Bayer, Biogen-Idec, Merck-Serono, Teva, Novartis, Actelion, Allergan, Almirall, Sanofi-Genzyme and Roche. E. Martín-Montañez received honoraria as consultant in advisory boards by Novartis. The remaining authors declare no competing interests.

Bibliography

[1] S.A. Doggrell, Oral fingolimod for relapsing-remitting multiple sclerosis, Expert Opin. Pharmacother. 11 (2010) 1777–1781. doi:10.1517/14656566.2010.481671.

[2] L. Kappos, E.-W. Radue, P. O'Connor, C. Polman, R. Hohlfeld, P. Calabresi, K. Selmaj, C. Agoropoulou, M. Leyk, L. Zhang-Auberson, P. Burtin, A Placebo-Controlled Trial of Oral Fingolimod in Relapsing Multiple Sclerosis, N. Engl. J. Med. 362 (2010) 387–401. doi:10.1056/NEJMoa0909494.

[3] B. Singer, A.P. Ross, K. Tobias, Oral fingolimod for the treatment of patients with relapsing forms of multiple sclerosis, Int. J. Clin. Pract. 65 (2011) 887–895. doi:10.1111/j.1742-1241.2011.02721.x.

[4] J. Chun, H.-P. Hartung, Mechanism of Action of Oral Fingolimod (FTY720) in Multiple Sclerosis, Clin. Neuropharmacol. 33 (2010) 91–101. doi:10.1097/WNF.0b013e3181cbf825.

[5] L. Zhi, P. Kim, B.D. Thompson, C. Pitsillides, A.J. Bankovich, S.-H. Yun, C.P. Lin, J.G. Cyster, M.X. Wu, FTY720 blocks egress of T cells in part by abrogation of their adhesion on the lymph node sinus., J. Immunol. 187 (2011) 2244–51. doi:10.4049/jimmunol.1100670.

[6] C.W. Lee, J.W. Choi, J. Chun, Neurological S1P signaling as an emerging mechanism of action of oral FTY720 (Fingolimod) in multiple sclerosis, Arch. Pharm. Res. 33 (2010) 1567–1574. doi:10.1007/s12272-010-1008-5.

[7] M. Tintore, A. Vidal-Jordana, J. Sastre-Garriga, Treatment of multiple sclerosis — success from bench to bedside, Nat. Rev. Neurol. 15 (2019) 53–58. doi:10.1038/s41582-018-0082-z.

[8] B. Balatoni, M.K. Storch, E.-M. Swoboda, V. Schönborn, A. Koziel, G.N. Lambrou, P.C. Hiestand, R. Weissert, C.A. Foster, FTY720 sustains and restores neuronal function in the DA rat model of MOG-induced experimental autoimmune encephalomyelitis, Brain Res. Bull. 74 (2007) 307–316. doi:10.1016/J.BRAINRESBULL.2007.06.023.

[9] M. Nazari, S. Keshavarz, A. Rafati, M.R. Namavar, M. Haghani, Fingolimod (FTY720) improves hippocampal synaptic plasticity and memory deficit in rats following focal cerebral ischemia, Brain Res. Bull. 124 (2016) 95–102. doi:10.1016/J.BRAINRESBULL.2016.04.004.

[10] R. Brunkhorst, N. Kanaan, A. Koch, N. Ferreirós, A. Mirceska, P. Zeiner, M. Mittelbronn, A. Derouiche, H. Steinmetz, C. Foerch, J. Pfeilschifter, W. Pfeilschifter, FTY720 Treatment in the Convalescence Period Improves Functional Recovery and Reduces Reactive Astrogliosis in Photothrombotic Stroke, PLoS One. 8 (2013). doi:10.1371/journal.pone.0070124.

[11] Y. Fu, N. Zhang, L. Ren, Y. Yan, N. Sun, Y.-J. Li, W. Han, R. Xue, Q. Liu,

J. Hao, C. Yu, F.-D. Shi, Impact of an immune modulator fingolimod on acute ischemic stroke., Proc. Natl. Acad. Sci. U. S. A. 111 (2014) 18315–20. doi:10.1073/pnas.1416166111.

[12] A. Miguez, G. García-Díaz Barriga, V. Brito, M. Straccia, A. Giralt, S. Ginés, J.M. Canals, J. Alberch, Fingolimod (FTY720) enhances hippocampal synaptic plasticity and memory in Huntington's disease by preventing p75 ^{NTR} up-regulation and astrocyte-mediated inflammation, Hum. Mol. Genet. 24 (2015) 4958–4970. doi:10.1093/hmg/ddv218.

[13] M. Asle-Rousta, Z. Kolahdooz, L. Dargahi, A. Ahmadiani, S. Nasoohi, Prominence of Central Sphingosine-1-Phosphate Receptor-1 in Attenuating Aβ-Induced Injury by Fingolimod, J. Mol. Neurosci. 54 (2014) 698–703. doi:10.1007/s12031-014-0423-3.

[14] M. Asle-Rousta, Z. Kolahdooz, S. Oryan, A. Ahmadiani, L. Dargahi, FTY720 (Fingolimod) Attenuates Beta-amyloid Peptide (Aβ42)-Induced Impairment of Spatial Learning and Memory in Rats, J. Mol. Neurosci. 50 (2013) 524–532. doi:10.1007/s12031-013-9979-6.

[15] A.J. Thompson, S.E. Baranzini, J. Geurts, B. Hemmer, O. Ciccarelli, Multiple sclerosis, Lancet. 391 (2018) 1622–1636. doi:10.1016/S0140-6736(18)30481-1.

[16] H. Lassmann, J. van Horssen, D. Mahad, Progressive multiple sclerosis: pathology and pathogenesis, Nat. Rev. Neurol. 8 (2012) 647–656. doi:10.1038/nrneurol.2012.168.

[17] J. van Horssen, G. Schreibelt, J. Drexhage, T. Hazes, C.D. Dijkstra, P. van der Valk, H.E. de Vries, Severe oxidative damage in multiple sclerosis lesions coincides with enhanced antioxidant enzyme expression, Free Radic. Biol. Med. 45 (2008) 1729–1737. doi:10.1016/J.FREERADBIOMED.2008.09.023.

[18] M.E. Witte, J.J.G. Geurts, H.E. de Vries, P. van der Valk, J. van Horssen, Mitochondrial dysfunction: A potential link between neuroinflammation and neurodegeneration?, Mitochondrion. 10 (2010) 411–418. doi:10.1016/J.MITO.2010.05.014.

[19] D. Johnson, E. Allman, K. Nehrke, Regulation of acid-base transporters by reactive oxygen species following mitochondrial fragmentation, Am. J. Physiol. Physiol. 302 (2012) C1045–C1054. doi:10.1152/ajpcell.00411.2011.

[20] S. Dröse, U. Brandt, Molecular Mechanisms of Superoxide Production by the Mitochondrial Respiratory Chain, in: Springer, New York, NY, 2012: pp. 145–169. doi:10.1007/978-1-4614-3573-0_6.

[21] S. Dröse, U. Brandt, I. Wittig, Mitochondrial respiratory chain complexes as sources and targets of thiol-based redox-regulation, Biochim. Biophys. Acta - Proteins Proteomics. 1844 (2014) 1344–1354. doi:10.1016/J.BBAPAP.2014.02.006.

[22] S. Franco-Iborra, M. Vila, C. Perier, Mitochondrial Quality Control in Neurodegenerative Diseases: Focus on Parkinson's Disease and

Huntington's Disease., Front. Neurosci. 12 (2018) 342. doi:10.3389/fnins.2018.00342.

[23] S. Srivastava, The Mitochondrial Basis of Aging and Age-Related Disorders., Genes (Basel). 8 (2017). doi:10.3390/genes8120398.

[24] A.N. Carvalho, J.L. Lim, P.G. Nijland, M.E. Witte, J. Van Horssen, Glutathione in multiple sclerosis: More than just an antioxidant?, Mult. Scler. J. 20 (2014) 1425–1431. doi:10.1177/1352458514533400.

[25] A. Neves Carvalho, O. Firuzi, M. Joao Gama, J. van Horssen, L. Saso, Oxidative Stress and Antioxidants in Neurological Diseases: Is There Still Hope?, Curr. Drug Targets. 18 (2017) 705–718. doi:10.2174/1389450117666160401120514.

[26] H.A. Elfawy, B. Das, Crosstalk between mitochondrial dysfunction, oxidative stress, and age related neurodegenerative disease: Etiologies and therapeutic strategies, Life Sci. 218 (2019) 165–184. doi:10.1016/j.lfs.2018.12.029.

[27] E. Gray, T.L. Thomas, S. Betmouni, N. Scolding, S. Love, Elevated myeloperoxidase activity in white matter in multiple sclerosis, Neurosci. Lett. 444 (2008) 195–198. doi:10.1016/J.NEULET.2008.08.035.

[28] B.D. Trapp, L. Bö, S. Mörk, A. Chang, Pathogenesis of tissue injury in MS lesions, J. Neuroimmunol. 98 (1999) 49–56. doi:10.1016/S0165-5728(99)00081-8.

[29] G.R. Campbell, J.T. Worrall, D.J. Mahad, The central role of mitochondria in axonal degeneration in multiple sclerosis, Mult. Scler. J. 20 (2014) 1806–1813. doi:10.1177/1352458514544537.

[30] M.T. Lin, M.F. Beal, Mitochondrial dysfunction and oxidative stress in neurodegenerative diseases, Nat. 2006 4437113. (2006).

[31] D.J. Mahad, I. Ziabreva, G. Campbell, N. Lax, K. White, P.S. Hanson, H. Lassmann, D.M. Turnbull, Mitochondrial changes within axons in multiple sclerosis, Brain. 132 (2009) 1161–1174. doi:10.1093/brain/awp046.

[32] D.H. Mahad, B.D. Trapp, H. Lassmann, Pathological mechanisms in progressive multiple sclerosis, Lancet Neurol. 14 (2015) 183–193. doi:10.1016/S1474-4422(14)70256-X.

[33] P. Mao, P.H. Reddy, Is multiple sclerosis a mitochondrial disease?, Biochim. Biophys. Acta - Mol. Basis Dis. 1802 (2010) 66–79. doi:10.1016/J.BBADIS.2009.07.002.

[34] J.H. Son, H.S. Chun, T.H. Joh, S. Cho, B. Conti, J.W. Lee, Neuroprotection and neuronal differentiation studies using substantia nigra dopaminergic cells derived from transgenic mouse embryos., J. Neurosci. 19 (1999) 10–20. doi:10.1523/JNEUROSCI.19-01-00010.1999.

[35] J.Y. Koh, D.W. Choi, Quantitative determination of glutamate mediated cortical neuronal injury in cell culture by lactate dehydrogenase efflux assay, J. Neurosci. Methods. 20 (1987) 83–90. doi:10.1016/0165-0270(87)90041-0.

[36] E. Martín-Montañez, C. Millon, F. Boraldi, F. Garcia-Guirado, C. Pedraza, E. Lara, L.J. Santin, J. Pavia, M. Garcia-Fernandez, IGF-II promotes neuroprotection and neuroplasticity recovery in a long-lasting model of oxidative damage induced by glucocorticoids, Redox Biol. 13 (2017) 69–81. doi:10.1016/J.REDOX.2017.05.012.

[37] M.E. Kauffman, M.K. Kauffman, K. Traore, H. Zhu, M.A. Trush, Z. Jia, Y.R. Li, MitoSOX-Based Flow Cytometry for Detecting Mitochondrial ROS., React. Oxyg. Species (Apex, N.C.). 2 (2016) 361–370. doi:10.20455/ros.2016.865.

[38] M.M. Bradford, A rapid and sensitive method for the quantitation of microgram quantities of protein utilizing the principle of protein-dye binding, Anal. Biochem. 72 (1976) 248–254. doi:10.1016/0003-2697(76)90527-3.

[39] C. Lind, E. Cadenas, P. Hochstein, L. Ernster, DT-diaphorase: Purification, properties, and function, Methods Enzymol. 186 (1990) 287–301. doi:10.1016/0076-6879(90)86122-C.

[40] M.I. Garcia-Fernandez, D. Gheduzzi, F. Boraldi, C.D. Paolinelli, P. Sanchez, P. Valdivielso, M.J. Morilla, D. Quaglino, D. Guerra, S. Casolari, L. Bercovitch, I. Pasquali-Ronchetti, Parameters of oxidative stress are present in the circulation of PXE patients, Biochim. Biophys. Acta - Mol. Basis Dis. 1782 (2008) 474–481. doi:10.1016/J.BBADIS.2008.05.001.

[41] I. Pasquali-Ronchetti, M.I. Garcia-Fernandez, F. Boraldi, D. Quaglino, D. Gheduzzi, C. De Vincenzi Paolinelli, R. Tiozzo, S. Bergamini, D. Ceccarelli, U. Muscatello, Oxidative stress in fibroblasts from patients with pseudoxanthoma elasticum: possible role in the pathogenesis of clinical manifestations, J. Pathol. 208 (2006) 54–61. doi:10.1002/path.1867.

[42] E. Martin-Montañez, J. Pavia, L.J. Santin, F. Boraldi, G. Estivill-Torrus, J.A. Aguirre, M. Garcia-Fernandez, Involvement of IGF-II receptors in the antioxidant and neuroprotective effects of IGF-II on adult cortical neuronal cultures, Biochim. Biophys. Acta - Mol. Basis Dis. 1842 (2014) 1041–1051. doi:10.1016/J.BBADIS.2014.03.010.

[43] J.Y. Heo, J.H. Park, S.J. Kim, K.S. Seo, J.S. Han, S.H. Lee, J.M. Kim, J. Il Park, S.K. Park, K. Lim, B.D. Hwang, M. Shong, G.R. Kweon, DJ-1 Null Dopaminergic Neuronal Cells Exhibit Defects in Mitochondrial Function and Structure: Involvement of Mitochondrial Complex I Assembly, PLoS One. 7 (2012) e32629. doi:10.1371/journal.pone.0032629.

[44] W. Pendergrass, N. Wolf, M. Poot, Efficacy of MitoTracker Green? and CMXrosamine to measure changes in mitochondrial membrane potentials in living cells and tissues, Cytometry. 61A (2004) 162–169. doi:10.1002/cyto.a.20033.

[45] D. Taverna, F. Boraldi, G. De Santis, R.M. Caprioli, D. Quaglino, Histology-directed and imaging mass spectrometry: An emerging technology in ectopic calcification., Bone. 74 (2015) 83–94. doi:10.1016/j.bone.2015.01.004.

[46] G.H. Kim, J.E. Kim, S.J. Rhie, S. Yoon, The Role of Oxidative Stress in Neurodegenerative Diseases., Exp. Neurobiol. 24 (2015) 325–40. doi:10.5607/en.2015.24.4.325.

[47] B. Uttara, A. V Singh, P. Zamboni, R.T. Mahajan, Oxidative stress and neurodegenerative diseases: a review of upstream and downstream antioxidant therapeutic options., Curr. Neuropharmacol. 7 (2009) 65–74. doi:10.2174/157015909787602823.

[48] K. Ohl, K. Tenbrock, M. Kipp, Oxidative stress in multiple sclerosis: Central and peripheral mode of action, Exp. Neurol. 277 (2016) 58–67. doi:10.1016/j.expneurol.2015.11.010.

[49] D. Offen, Y. Gilgun-Sherki, E. Melamed, The role of oxidative stress in the pathogenesis of multiple sclerosis: The need for effective antioxidant therapy, J. Neurol. 251 (2004) 261–268. doi:10.1007/s00415-004-0348-9.

[50] G. Loor, J. Kondapalli, J.M. Schriewer, N.S. Chandel, T.L. Vanden Hoek, P.T. Schumacker, Menadione triggers cell death through ROS-dependent mechanisms involving PARP activation without requiring apoptosis., Free Radic. Biol. Med. 49 (2010) 1925–36. doi:10.1016/j.freeradbiomed.2010.09.021.

[51] A. Ashkenazi, G. Salvesen, Regulated Cell Death: Signaling and Mechanisms, Annu. Rev. Cell Dev. Biol. 30 (2014) 337–356. doi:10.1146/annurev-cellbio-100913-013226.

[52] L. Galluzzi, I. Vitale, S.A. Aaronson, J.M. Abrams, D. Adam, P. Agostinis, E.S. Alnemri, L. Altucci, I. Amelio, D.W. Andrews, M. Annicchiarico-Petruzzelli, A. V Antonov, E. Arama, E.H. Baehrecke, N.A. Barlev, N.G. Bazan, F. Bernassola, M.J.M. Bertrand, K. Bianchi, M. V Blagosklonny, K. Blomgren, C. Borner, P. Boya, C. Brenner, M. Campanella, E. Candi, D. Carmona-Gutierrez, F. Cecconi, F.K.-M. Chan, N.S. Chandel, E.H. Cheng, J.E. Chipuk, J.A. Cidlowski, A. Ciechanover, G.M. Cohen, M. Conrad, J.R. Cubillos-Ruiz, P.E. Czabotar, V. D'Angiolella, T.M. Dawson, V.L. Dawson, V. De Laurenzi, R. De Maria, K.-M. Debatin, R.J. DeBerardinis, M. Deshmukh, N. Di Daniele, F. Di Virgilio, V.M. Dixit, S.J. Dixon, C.S. Duckett, B.D. Dynlacht, W.S. El-Deiry, J.W. Elrod, G.M. Fimia, S. Fulda, A.J. García-Sáez, A.D. Garg, C. Garrido, E. Gavathiotis, P. Golstein, E. Gottlieb, D.R. Green, L.A. Greene, H. Gronemeyer, A. Gross, G. Hajnoczky, J.M. Hardwick, I.S. Harris, M.O. Hengartner, C. Hetz, H. Ichijo, M. Jäättelä, B. Joseph, P.J. Jost, P.P. Juin, W.J. Kaiser, M. Karin, T. Kaufmann, O. Kepp, A. Kimchi, R.N. Kitsis, D.J. Klionsky, R.A. Knight, S. Kumar, S.W. Lee, J.J. Lemasters, B. Levine, A. Linkermann, S.A. Lipton, R.A. Lockshin, C. López-Otín, S.W. Lowe, T. Luedde, E. Lugli, M. MacFarlane, F. Madeo, M. Malewicz, W. Malorni, G. Manic, J.-C. Marine, S.J. Martin, J.-C. Martinou, J.P. Medema, P. Mehlen, P. Meier, S. Melino, E.A. Miao, J.D. Molkentin, U.M. Moll, C. Muñoz-Pinedo, S. Nagata, G. Nuñez, A. Oberst, M. Oren, M. Overholtzer, M. Pagano, T. Panaretakis, M. Pasparakis, J.M. Penninger, D.M. Pereira, S. Pervaiz, M.E. Peter, M. Piacentini, P. Pinton, J.H.M. Prehn, H. Puthalakath, G.A. Rabinovich, M. Rehm, R. Rizzuto, C.M.P. Rodrigues, D.C. Rubinsztein, T. Rudel, K.M. Ryan, E. Sayan, L. Scorrano, F. Shao,

Y. Shi, J. Silke, H.-U. Simon, A. Sistigu, B.R. Stockwell, A. Strasser, G. Szabadkai, S.W.G. Tait, D. Tang, N. Tavernarakis, A. Thorburn, Y. Tsujimoto, B. Turk, T. Vanden Berghe, P. Vandenabeele, M.G. Vander Heiden, A. Villunger, H.W. Virgin, K.H. Vousden, D. Vucic, E.F. Wagner, H. Walczak, D. Wallach, Y. Wang, J.A. Wells, W. Wood, J. Yuan, Z. Zakeri, B. Zhivotovsky, L. Zitvogel, G. Melino, G. Kroemer, Molecular mechanisms of cell death: recommendations of the Nomenclature Committee on Cell Death 2018., Cell Death Differ. 25 (2018) 486–541. doi:10.1038/s41418-017-0012-4.

[53] D. Ofengeim, Y. Ito, A. Najafov, Y. Zhang, B. Shan, J.P. DeWitt, J. Ye, X. Zhang, A. Chang, H. Vakifahmetoglu-Norberg, J. Geng, B. Py, W. Zhou, P. Amin, J.B. Lima, C. Qi, Q. Yu, B. Trapp, J. Yuan, Activation of Necroptosis in Multiple Sclerosis, Cell Rep. 10 (2015) 1836–1849. doi:10.1016/J.CELREP.2015.02.051.

[54] C. Hu, M. Nydes, K.L. Shanley, I.E. Morales Pantoja, T.A. Howard, O.A. Bizzozero, Reduced expression of the ferroptosis inhibitor glutathione peroxidase-4 in multiple sclerosis and experimental autoimmune encephalomyelitis, J. Neurochem. 148 (2019) 426–439. doi:10.1111/jnc.14604.

[55] K. Aoyama, T. Nakaki, Impaired glutathione synthesis in neurodegeneration., Int. J. Mol. Sci. 14 (2013) 21021–44. doi:10.3390/ijms141021021.

[56] B. Adamczyk, S. Wawrzyniak, S. Kasperczyk, M. Adamczyk-Sowa, The Evaluation of Oxidative Stress Parameters in Serum Patients with Relapsing-Remitting Multiple Sclerosis Treated with II-Line Immunomodulatory Therapy, Oxid. Med. Cell. Longev. 2017 (2017) 1–12. doi:10.1155/2017/9625806.

[57] E. Fetisova, B. Chernyak, G. Korshunova, M. Muntyan, V. Skulachev, Mitochondria-targeted Antioxidants as a Prospective Therapeutic Strategy for Multiple Sclerosis, Curr. Med. Chem. 24 (2017). doi:10.2174/0929867324666170316114452.

[58] M.E. Witte, D.J. Mahad, H. Lassmann, J. van Horssen, Mitochondrial dysfunction contributes to neurodegeneration in multiple sclerosis, Trends Mol. Med. 20 (2014) 179–187. doi:10.1016/J.MOLMED.2013.11.007.

[59] J.R. Lovas, X. Wang, The meaning of mitochondrial movement to a neuron's life., Biochim. Biophys. Acta. 1833 (2013) 184–94. doi:10.1016/j.bbamcr.2012.04.007.

[60] V.K. Rao, E.A. Carlson, S.S. Yan, Mitochondrial permeability transition pore is a potential drug target for neurodegeneration., Biochim. Biophys. Acta. 1842 (2014) 1267–72. doi:10.1016/j.bbadis.2013.09.003.

[61] M. Hüttemann, S. Helling, T.H. Sanderson, C. Sinkler, L. Samavati, G. Mahapatra, A. Varughese, G. Lu, J. Liu, R. Ramzan, S. Vogt, L.I. Grossman, J.W. Doan, K. Marcus, I. Lee, Regulation of mitochondrial respiration and apoptosis through cell signaling: Cytochrome c oxidase and cytochrome c in ischemia/reperfusion injury and inflammation,

Biochim. Biophys. Acta - Bioenerg. 1817 (2012) 598–609. doi:10.1016/J.BBABIO.2011.07.001.

[62] J. Teixeira, R. Amorim, K. Santos, P. Soares, S. Datta, G.A. Cortopassi, T.L. Serafim, V.A. Sardão, J. Garrido, F. Borges, P.J. Oliveira, Disruption of mitochondrial function as mechanism for anti-cancer activity of a novel mitochondriotropic menadione derivative, Toxicology. 393 (2018) 123–139. doi:10.1016/J.TOX.2017.11.014.

[63] F. Aboul-Enein, H. Rauschka, B. Kornek, C. Stadelmann, A. Stefferl, W. Brück, C. Lucchinetti, M. Schmidbauer, K. Jellinger, H. Lassmann, Preferential Loss of Myelin-Associated Glycoprotein Reflects Hypoxia-Like White Matter Damage in Stroke and Inflammatory Brain Diseases, J. Neuropathol. Exp. Neurol. 62 (2003) 25–33. doi:10.1093/jnen/62.1.25.

[64] S. Arnold, Cytochrome c Oxidase and Its Role in Neurodegeneration and Neuroprotection, in: Springer, New York, NY, 2012: pp. 305–339. doi:10.1007/978-1-4614-3573-0_13.

[65] S. O'Sullivan, Sphingosine-1-phosphate receptor therapies: Advances in clinical trials for CNS-related diseases, Neuropharmacology. 113 (2017) 597–607. doi:10.1016/J.NEUROPHARM.2016.11.006.

[66] G.M. Strub, M. Paillard, J. Liang, L. Gomez, J.C. Allegood, N.C. Hait, M. Maceyka, M.M. Price, Q. Chen, D.C. Simpson, T. Kordula, S. Milstien, E.J. Lesnefsky, S. Spiegel, Sphingosine-1-phosphate produced by sphingosine kinase 2 in mitochondria interacts with prohibitin 2 to regulate complex IV assembly and respiration, FASEB J. 25 (2011) 600–612. doi:10.1096/fj.10-167502.

[67] A. Mendoza, V. Fang, C. Chen, M. Serasinghe, A. Verma, J. Muller, V.S. Chaluvadi, M.L. Dustin, T. Hla, O. Elemento, J.E. Chipuk, S.R. Schwab, Lymphatic endothelial S1P promotes mitochondrial function and survival in naive T cells, Nature. 546 (2017) 158–161. doi:10.1038/nature22352.

[68] J. Motyl, J.B. Strosznajder, Sphingosine kinase 1/sphingosine-1-phosphate receptors dependent signalling in neurodegenerative diseases. The promising target for neuroprotection in Parkinson's disease, Pharmacol. Reports. 70 (2018) 1010–1014. doi:10.1016/J.PHAREP.2018.05.002.

[69] D. Mahad, I. Ziabreva, H. Lassmann, D. Turnbull, Mitochondrial defects in acute multiple sclerosis lesions., Brain. 131 (2008) 1722–35. doi:10.1093/brain/awn105.

[70] A. Bajwa, D.L. Rosin, P. Chroscicki, S. Lee, K. Dondeti, H. Ye, G.R. Kinsey, B.K. Stevens, K. Jobin, B.M. Kenwood, K.L. Hoehn, K.R. Lynch, M.D. Okusa, Sphingosine 1-Phosphate Receptor-1 Enhances Mitochondrial Function and Reduces Cisplatin-Induced Tubule Injury, J. Am. Soc. Nephrol. 26 (2015) 908–925. doi:10.1681/ASN.2013121351.

[71] R. Ghasemi, L. Dargahi, A. Ahmadiani, Integrated sphingosine-1 phosphate signaling in the central nervous system: From physiological equilibrium to pathological damage, Pharmacol. Res. 104 (2016) 156–

164. doi:10.1016/J.PHRS.2015.11.006.

[72] A. Mancini, L. Gaetani, L. Gentili, M. Di Filippo, Finding a way to preserve mitochondria: new pathogenic pathways in experimental multiple sclerosis, Neural Regen. Res. 14 (2019) 77–78. doi:10.4103/1673-5374.243707.

[73] N. Esteras, A.T. Dinkova-Kostova, A.Y. Abramov, Nrf2 activation in the treatment of neurodegenerative diseases: a focus on its role in mitochondrial bioenergetics and function, Biol. Chem. 397 (2016) 383–400. doi:10.1515/hsz-2015-0295.

[74] A.T. Dinkova-Kostova, A.Y. Abramov, The emerging role of Nrf2 in mitochondrial function, Free Radic. Biol. Med. 88 (2015) 179–188. doi:10.1016/J.FREERADBIOMED.2015.04.036.

[75] A. Cuadrado, NRF2 in neurodegenerative diseases, Curr. Opin. Toxicol. 1 (2016) 46–53. doi:10.1016/J.COTOX.2016.09.004.

[76] I.E. Morales-Pantoja, C. Hu, N.I. Perrone-Bizzozero, J. Zheng, O.A. Bizzozero, Nrf2-dysregulation correlates with reduced synthesis and low glutathione levels in experimental autoimmune encephalomyelitis, J. Neurochem. 139 (2016) 640. doi:10.1111/JNC.13837.

[77] S.K. Niture, R. Khatri, A.K. Jaiswal, Regulation of Nrf2-an update., Free Radic. Biol. Med. 66 (2014) 36–44. doi:10.1016/j.freeradbiomed.2013.02.008.

[78] G. Covas, H.S. Marinho, L. Cyrne, F. Antunes, Activation of Nrf2 by H2O2: De Novo Synthesis Versus Nuclear Translocation, Methods Enzymol. 528 (2013) 157–171. doi:10.1016/B978-0-12-405881-1.00009-4.

[79] A.T. Dinkova-Kostova, R. V. Kostov, A.G. Kazantsev, The role of Nrf2 signaling in counteracting neurodegenerative diseases, FEBS J. 285 (2018) 3576–3590. doi:10.1111/febs.14379.

[80] A.P. Mazzetti, M.C. Fiorile, A. Primavera, M. Lo Bello, Glutathione transferases and neurodegenerative diseases, Neurochem. Int. 82 (2015) 10–18. doi:10.1016/j.neuint.2015.01.008.

[81] J. van Horssen, M.E. Witte, G. Schreibelt, H.E. de Vries, Radical changes in multiple sclerosis pathogenesis, Biochim. Biophys. Acta - Mol. Basis Dis. 1812 (2011) 141–150. doi:10.1016/J.BBADIS.2010.06.011.

[82] C. Higashi, A. Kawaji, N. Tsuda, M. Hayashi, R. Saito, Y. Yagishita, T. Suzuki, A. Uruno, M. Nakamura, K. Nakao, S. Furusako, M. Yamamoto, The novel Nrf2 inducer TFM-735 ameliorates experimental autoimmune encephalomyelitis in mice, Eur. J. Pharmacol. 802 (2017) 76–84. doi:10.1016/J.EJPHAR.2017.02.044.

[83] N. Allocati, M. Masulli, C. Di Ilio, L. Federici, Glutathione transferases: substrates, inihibitors and pro-drugs in cancer and neurodegenerative diseases, Oncogenesis. 7 (2018) 8. doi:10.1038/s41389-017-0025-3.

[84] H.M. Schipper, W. Song, H. Zukor, J.R. Hascalovici, D. Zeligman, Heme

oxygenase-1 and neurodegeneration: expanding frontiers of engagement, J. Neurochem. 110 (2009) 469–485. doi:10.1111/j.1471-4159.2009.06160.x.

[85] E. Holzerova, K. Danhauser, T.B. Haack, L.S. Kremer, M. Melcher, I. Ingold, S. Kobayashi, C. Terrile, P. Wolf, J. Schaper, E. Mayatepek, F. Baertling, J.P. Friedmann Angeli, M. Conrad, T.M. Strom, T. Meitinger, H. Prokisch, F. Distelmaier, Human thioredoxin 2 deficiency impairs mitochondrial redox homeostasis and causes early-onset neurodegeneration, Brain. 139 (2016) 346–354. doi:10.1093/brain/awv350.

[86] G.J. McBean, M. Aslan, H.R. Griffiths, R.C. Torrão, Thiol redox homeostasis in neurodegenerative disease., Redox Biol. 5 (2015) 186–94. doi:10.1016/j.redox.2015.04.004.

[87] K.A.O. Gandy, L.M. Obeid, Regulation of the Sphingosine Kinase/Sphingosine 1-Phosphate Pathway, in: Springer, Vienna, 2013: pp. 275–303. doi:10.1007/978-3-7091-1511-4_14.

[88] G. Novi, A. Ghezzi, M. Pizzorno, C. Lapucci, F. Bandini, P. Annovazzi, G.L. Mancardi, A. Uccelli, Dramatic rebounds of MS during pregnancy following fingolimod withdrawal., Neurol. Neuroimmunol. Neuroinflammation. 4 (2017) e377. doi:10.1212/NXI.0000000000000377.

[89] M.E. Evangelopoulos, A. Miclea, L. Schrewe, M. Briner, A. Salmen, B. Engelhardt, A. Huwiler, A. Chan, R. Hoepner, Frequency and clinical characteristics of Multiple Sclerosis rebounds after withdrawal of Fingolimod, CNS Neurosci. Ther. (2018). doi:10.1111/cns.12992.

[90] G. Campbell, D.J. Mahad, Mitochondrial dysfunction and axon degeneration in progressive multiple sclerosis, FEBS Lett. 592 (2018) 1113–1121. doi:10.1002/1873-3468.13013.

[91] M. Sivasubramanian, N. Kanagaraj, S.T. Dheen, S.S.W. Tay, Sphingosine kinase 2 and sphingosine-1-phosphate promotes mitochondrial function in dopaminergic neurons of mouse model of Parkinson's disease and in MPP+-treated MN9D cells in vitro, Neuroscience. 290 (2015) 636–648. doi:10.1016/J.NEUROSCIENCE.2015.01.032.

Figures and captions

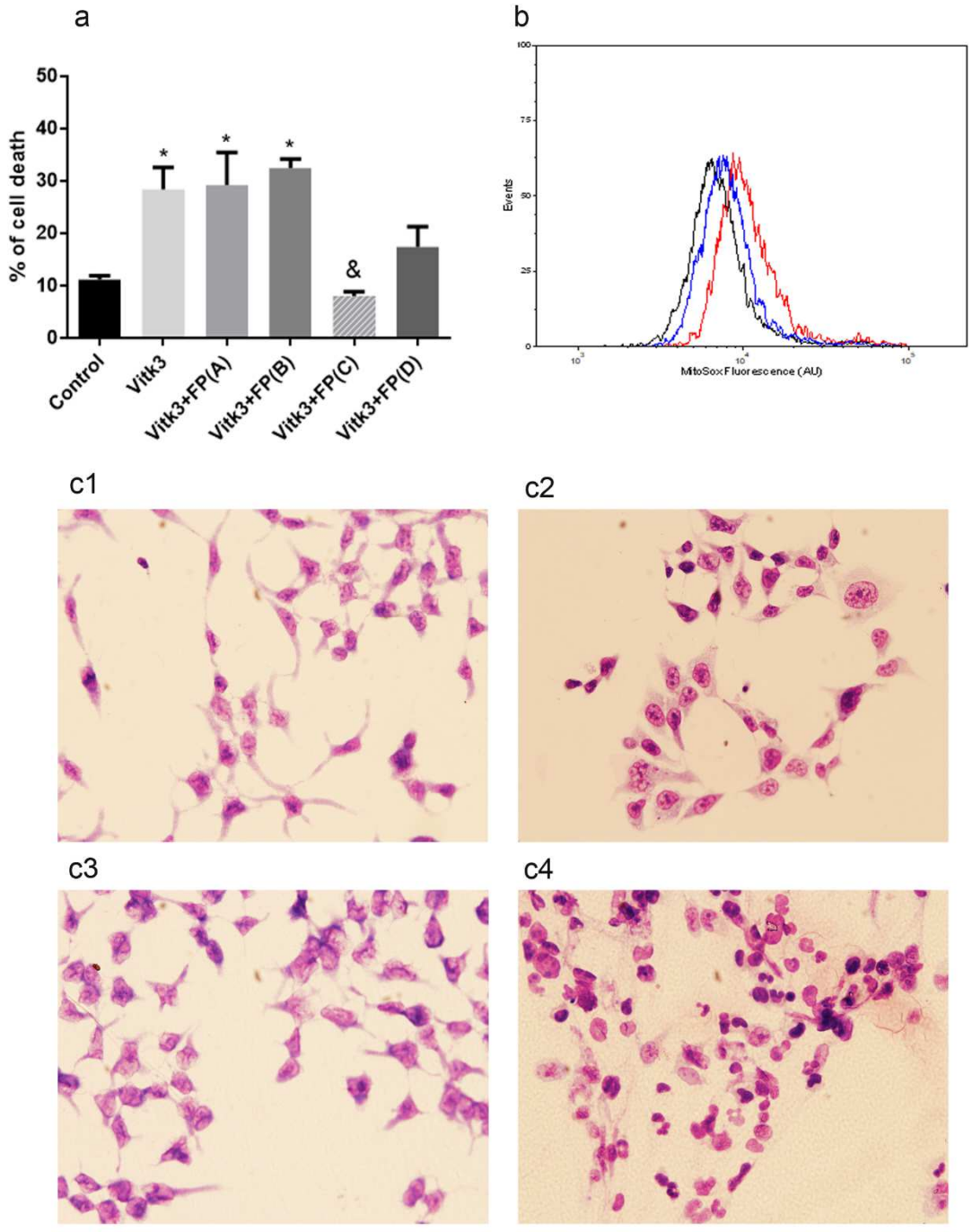

Figure 1. Cell death and mitochondrial ROS production in SN4741 neuronal cells after four hours of incubation with 15 µM Vitk3 in presence or absence of 50 nM FP. Panel a shows the effect on cellular viability of Vitk3 alone and co-incubated with different concentration of FP (A: 0.1 nM; B: 10 nM; C: 50nM; D: 100 nM). Data were combined from 3 to 5 independent experiments and presented as mean ± SEM. * $p<0.05$ compared to control cells, & $p<0.05$ compared with Vitk3 incubated cells. Panel b shows the mitochondrial ROS production displayed by MitoSOX staining (Black line: Control; Red line: Vitk3; Blue line: Vitk3+FP). Panel c shows Giemsa staining of different situations (c1: control cells; c2: Vitk3 treated cells; c3: Vitk3 in presence of 50 nM FP and c4: Vitk3 in presence of 50 nM FP and 10 µM W123).

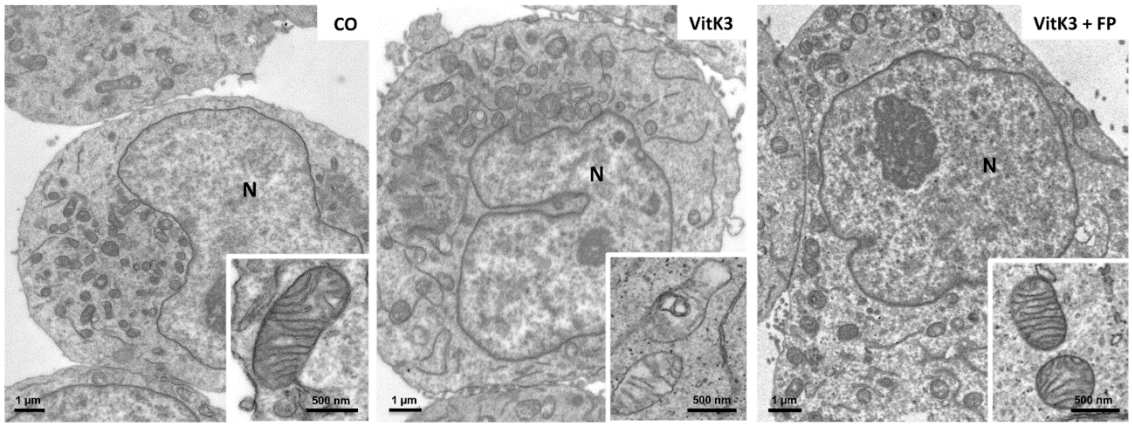

Figure 2. Ultrastructural appearances of SN4741 dopaminergic cells untreated (CO), treated with 15 µM of VitK3 (Vitk3) or VitK3 in presence of 50 nM FP (Vitk3+FP) for 4 hours.

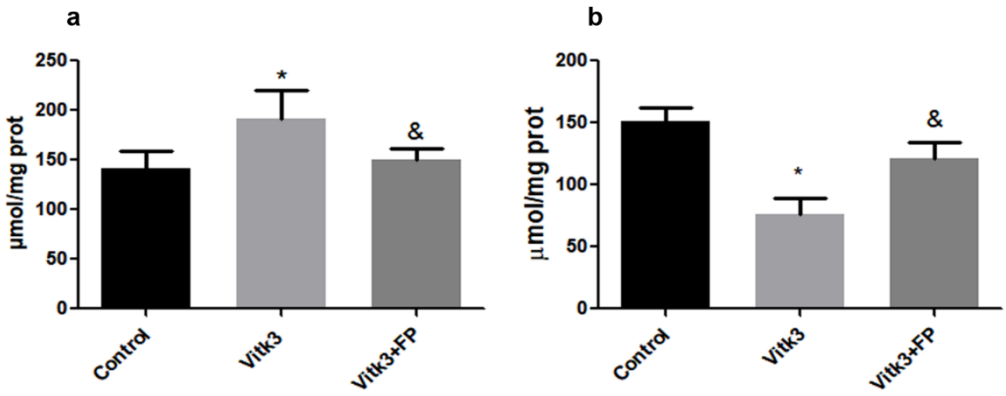

Figure 3. REDOX balance after four hours of incubation with 15 µM Vitk3 in presence or absence of 50 nM FP. Panel a shows the levels of advanced oxidation protein products and panel b shows the level of total thiols after different treatment conditions. The data represent mean ± SEM from 3 to 4 independent experiments (*$p<0.05$ versus control; & $p<0.05$ versus Vitk3).

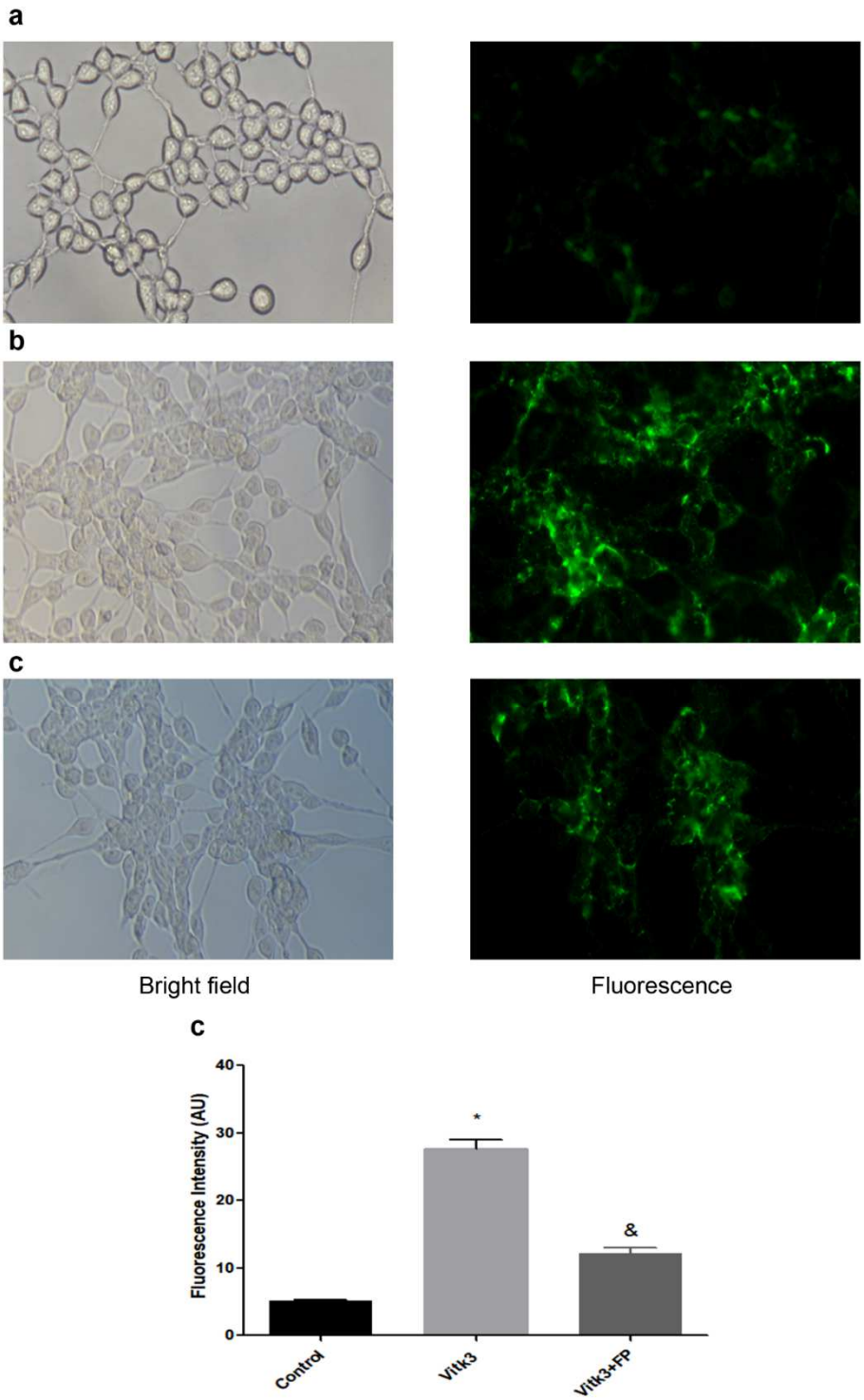

Figure 4. Caspase 3 activation induced by four hour of incubation with 15 µM Vitk3 in presence or absence of 50 nM FP. Representative images (20X) of NucView® 488 staining (a: Control; b: Vitk3; c: Vitk3+FP; d: Quantification of fluorescence intensity). Data were combined from 3 to 5 independent experiments and presented as mean ± SEM. * $p<0.05$ compared to control cells, & $p<0.05$ compared with Vitk3 incubated cells.

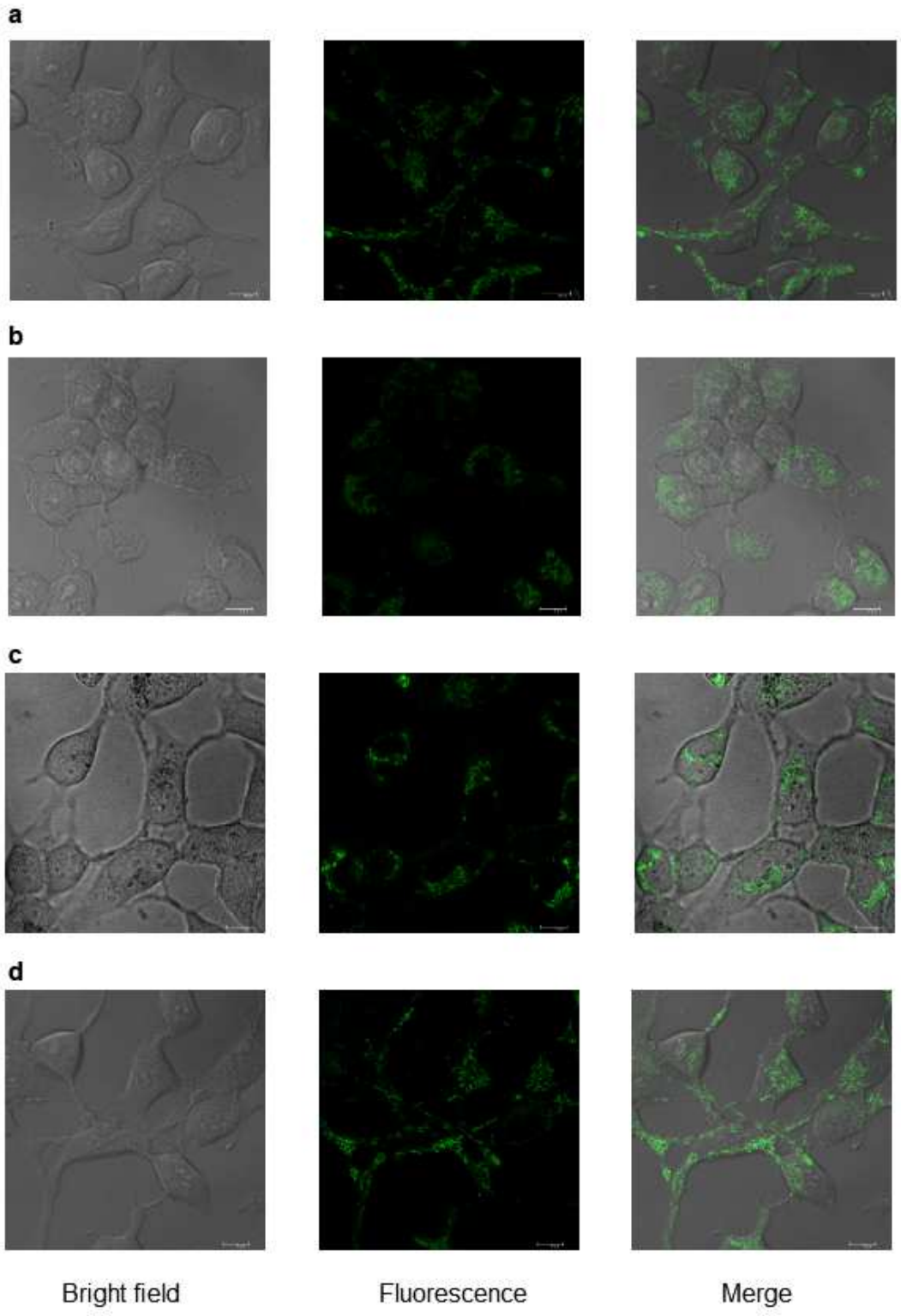

Figure 5: Confocal images of mitochondrial staining in neuronal cells with MitoTracker™ Green FM. Representative images after four hours of incubation with different substances (a: Control; b: Vitk3 15 µM; c: Vitk3 + 50nM FP; d: 50 nM FP).

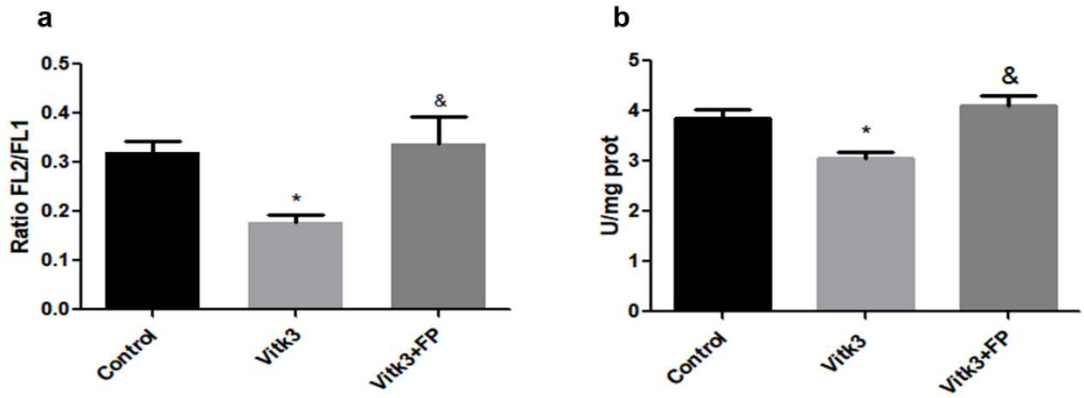

Figure 6: Cytofluorometric analysis of the MMP and COX activity after four hours of incubation with 15 µM Vitk3 in presence or absence of 50 nM FP. Panel a represents the fluorescence ratio of potential sensitive probe JC1. Panel b shows COX activity. Data were combined from 3 to 4 independent experiments and presented as mean ± SEM. (*$p<0.05$ versus control; & $p<0.05$ versus Vitk3).

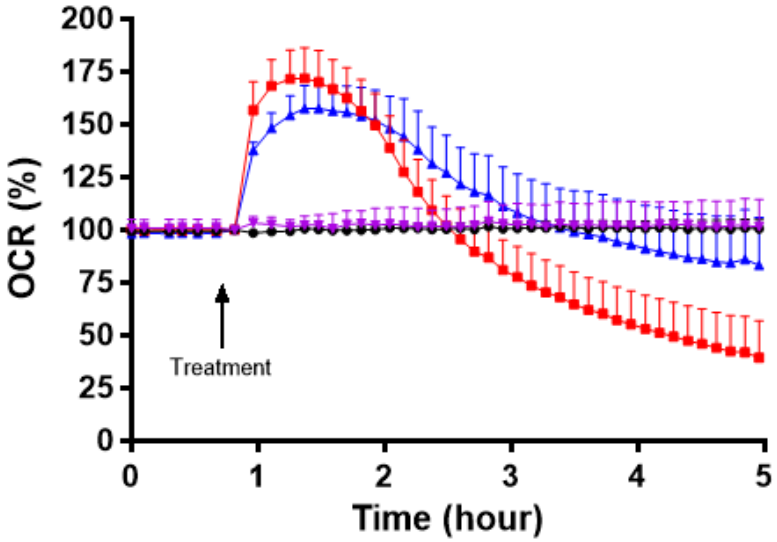

Figure 7. Time course of the effect of FP 50 nM on oxygen consumption rate after incubation with 15 µM VitK3 in presence or absence of FP. (Black line: Control; Red line: Vitk3; Blue line: Vitk3+FP; Purple line: FP).

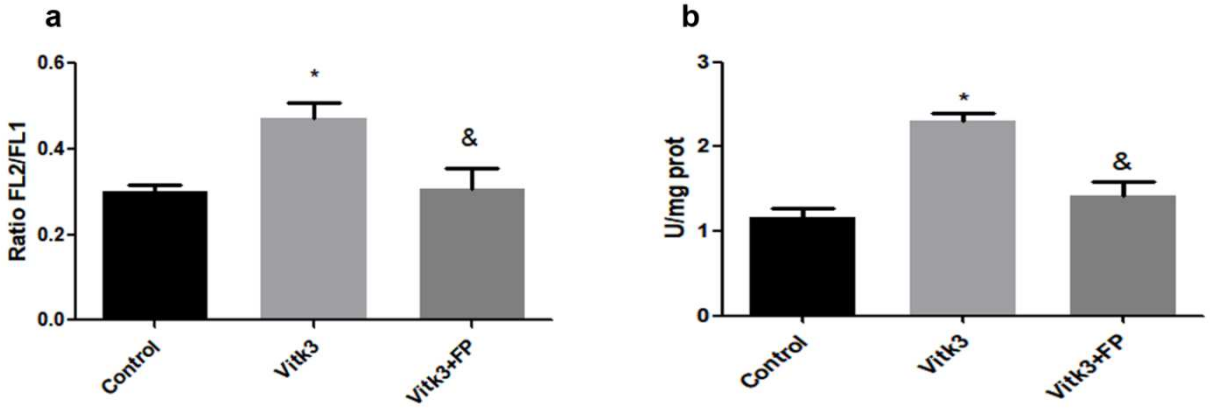

Figure 8: MMP and COX activity in neuronal cells incubated two hours with 15µM Vitk3 in absence or presence of 50 nM FP. Panel a represents fluorescence ratio of JC1 staining and panel b COX activity. Data were combined from 3 to 5 independent experiments and presented as mean ± SEM (* $p<0.05$ versus control; & $p<0.05$ versus Vitk3).

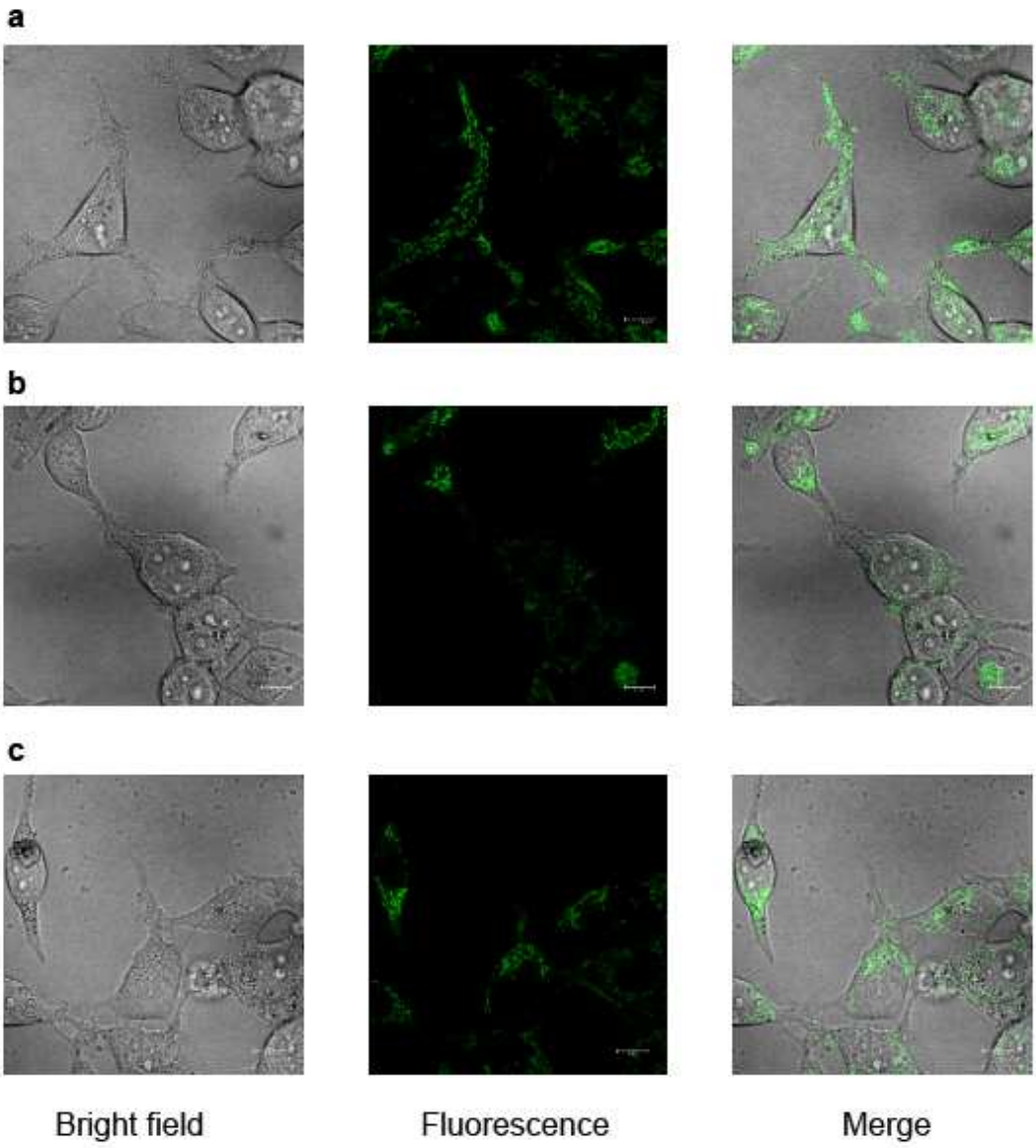

Figure 9. Confocal images of mitochondrial staining in neuronal cells with MitoTracker™ Green FM. Representative images after two hours of incubation with different substances (a: Control; b: Vitk3 15µM; c: Vitk3+50 nM FP).

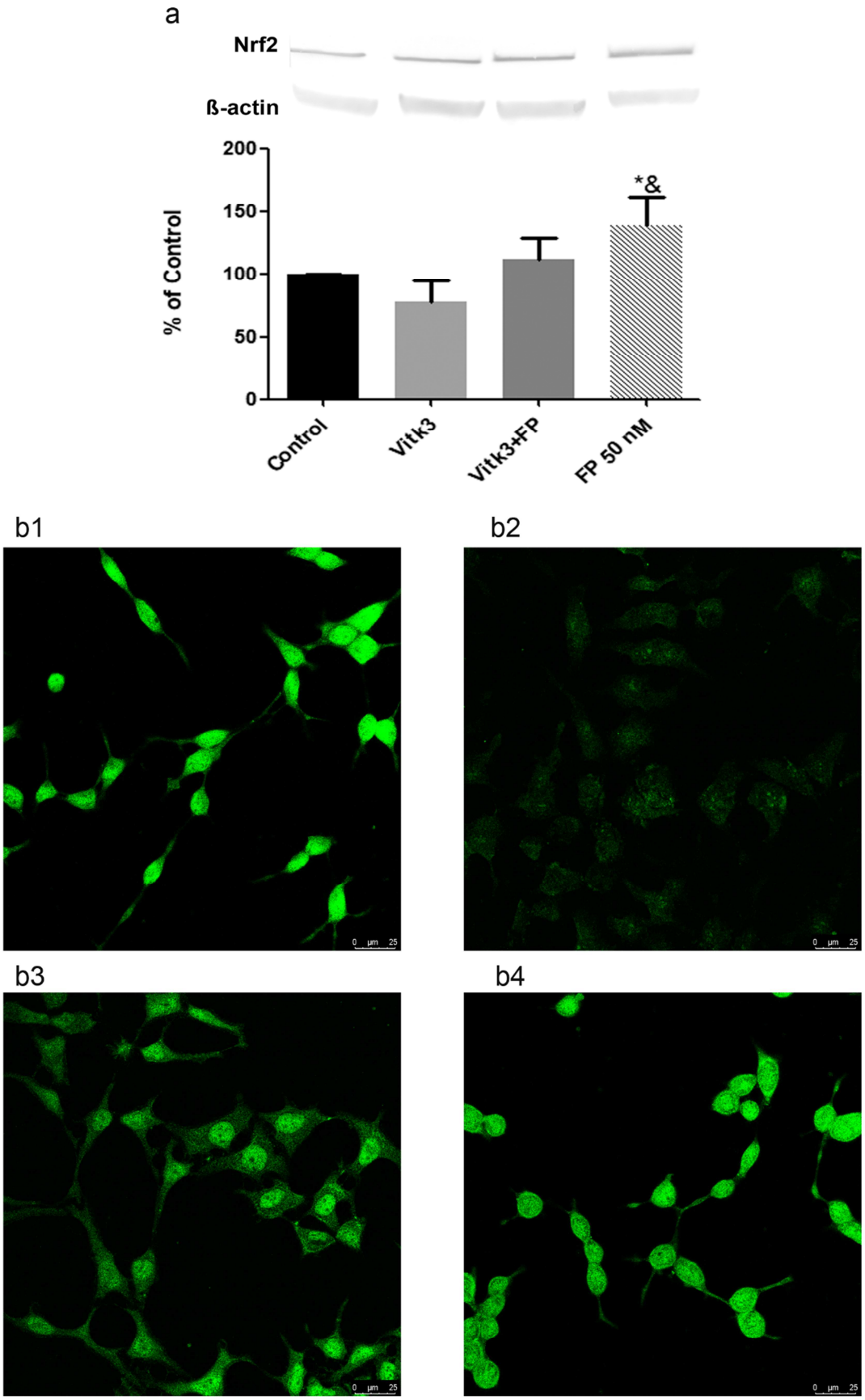

Figure 10. Nrf2 expression after four hours of incubation with 15 µM Vitk3 in absence and presence of 50 nM FP. a: Representative Western blot and quantification after normalising with β-actin; data were combined from 3 to 4 independent experiments and presented as mean ± SEM. (* $p<0.05$ versus control0; & $p<0.05$ versus Vitk3). b: immunocytochemistry (b1: control cells; b2: Vitk3 treated cells; b3: Vitk3 in presence of 50 nM FP and b4: 50 nM FP).

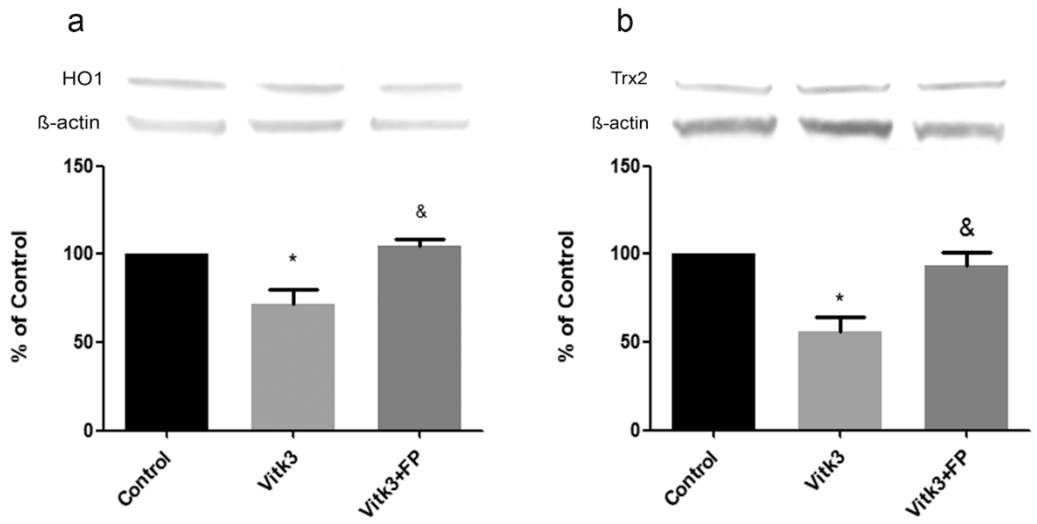

Figure 11. Expression of HO1 (panel a) and Trx2 (panel b) after four hours of incubation with 15 µM Vitk3 in presence or absence of 50 nM FP. Representative Western blots (upper panels) and quantifications after normalising with β-actin (lower panels). In lower panels, data were combined from 4 to 5 independent experiments and presented as mean ± SEM. (* $p<0.05$ versus control; & $p<0.05$ versus Vitk3).

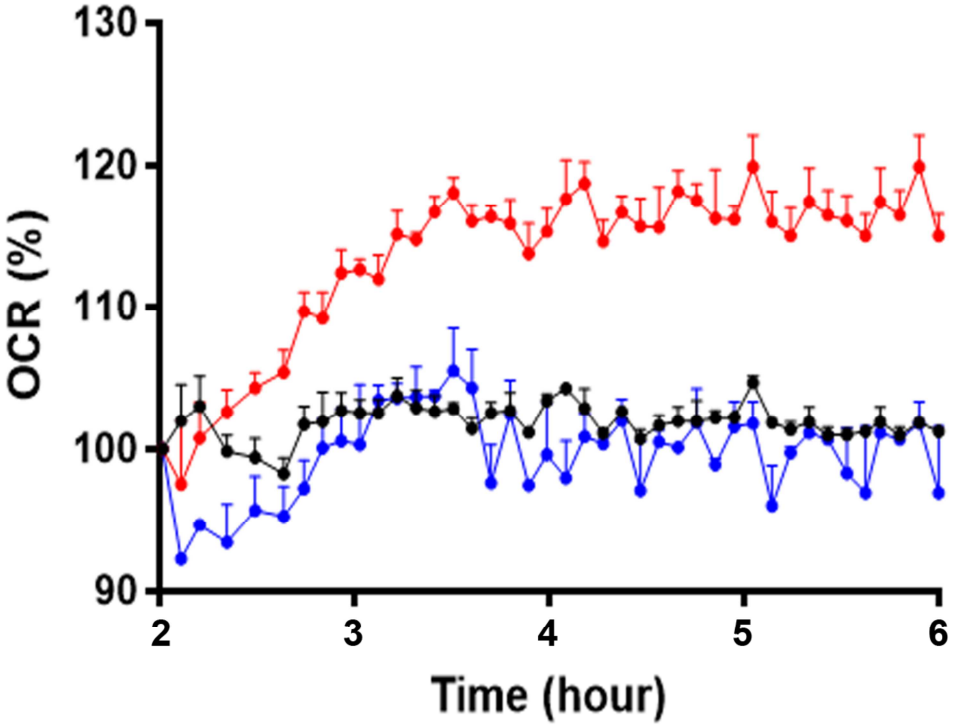

Figure 12: Time course of the effect of 50 nM FP on oxygen consume rate after two hours of incubation with 5 µM Vitk3 in presence or absence of FP. After two hours of incubation Vitk3 was removed from the media and cells were incubated for four additional hours in the following conditions: two groups were incubated with media (Vitk3 and control) and one with FP 50nM (Black line: Control; Red line: Vitk3; Blue line: Vitk3+FP).

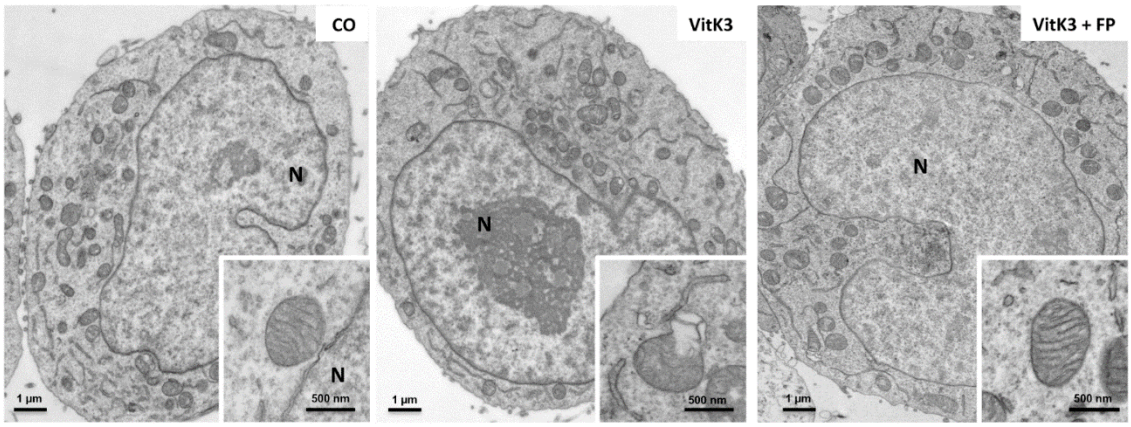

Figure 13. Ultrastructural appearances of SN4741 dopaminergic cells untreated (CO), treated with 5 µM of VitK3 (Vitk3) or VitK3 in presence of 50 nM FP (Vitk3+FP) for 2 hours. After two hours of incubation, Vitk3 was removed from the media and cells were incubated for two additional hours in the following conditions: two groups were incubated with media (Vitk3 and control) and one with FP 50nM.

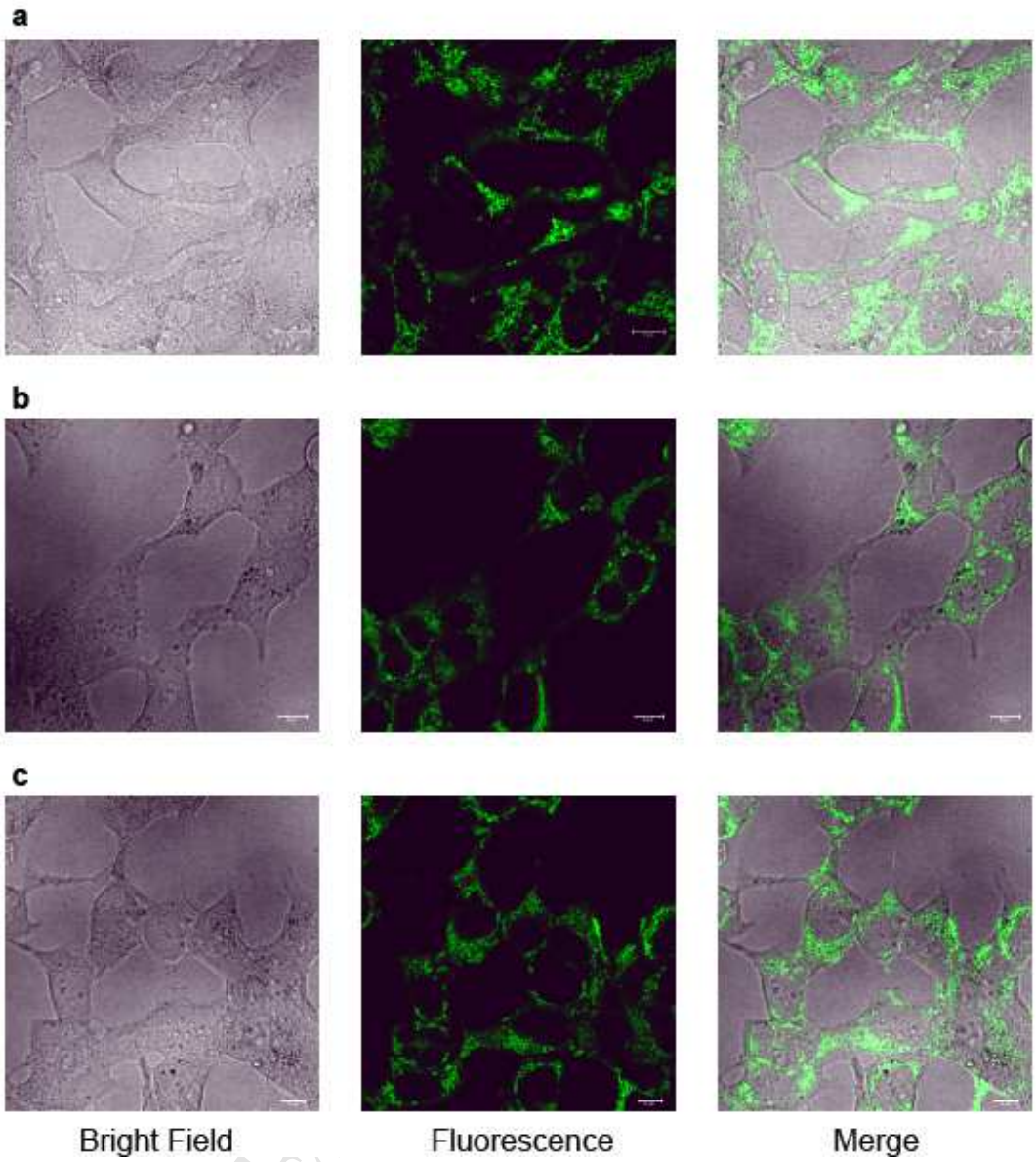

Figure 14. Confocal representative images of mitochondrial staining of neuronal cells with MitoTracker™ Green FM. After two hours of incubation with 5 µM Vitk3 in presence or absence of 50 nM FP, substances were removed from the media and cells were incubated for two additional hours in the following conditions: two groups were incubated with media (Vitk3 and control) and one with FP 50nM (a: Control; b: Vitk3 15µM; c: Vitk3+50 nM FP).

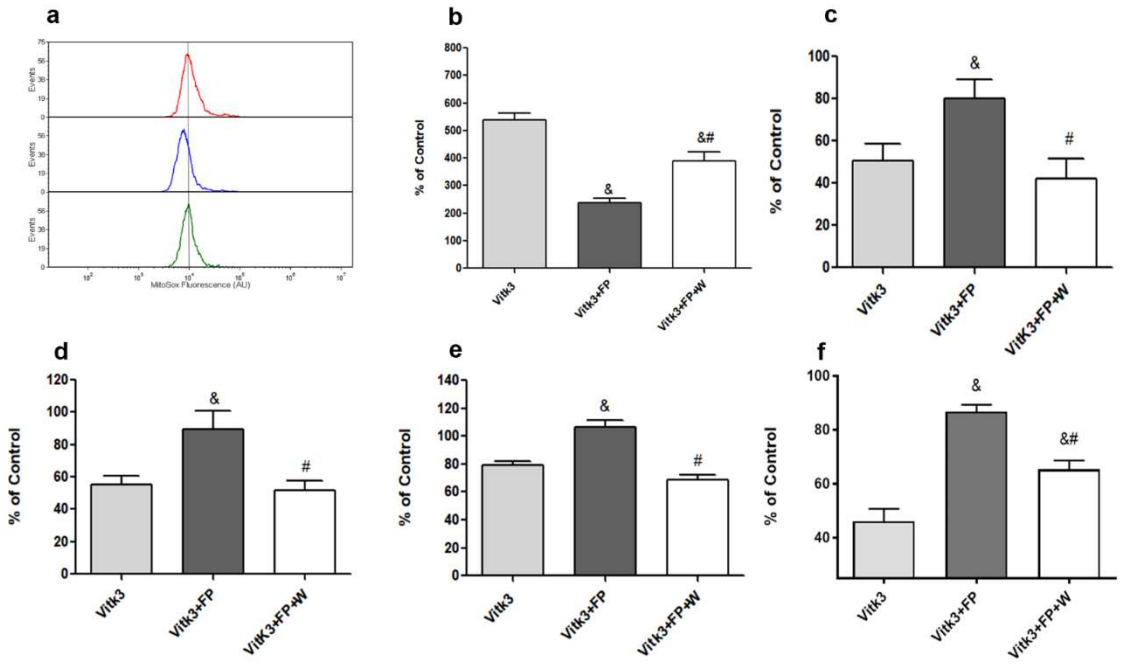

Figure 15. Effect of 10 µM of the S1P antagonist W123 on different parameters of mitochondrial oxidative damage induced by 15 µM Vitk3 in presence or absence of 50 nM FP (a: representative histograms of mitochondrial ROS production (red: Vitk3; blue: Vitk3+FP; green: Vitk3+FP+W123); b: Caspase 3 activation; c: total thiol levels; d: MMP; e: COX activity and f: OCR). Data were combined from 4 to 5 independent experiments and presented as mean ± SEM. (& $p<0.05$ versus Vitk3, # $p<0.05$ versus Vitk3+FP).

Highlights

First evidence of fingolimod phosphate protection against oxidative damage in neurons.

Fingolimod phosphate recovers mitochondrial function in neuronal cells after oxidative damage.

Fingolimod phosphate restores mitochondrial distribution in neurons after oxidative damage.

S1P receptors are involved in the recovery of neuronal mitochondrial function after oxidative damage.